AGU PUBLICATIONS

JGR

Journal of Geophysical Research: Solid Earth

RESEARCH ARTICLE

10.1002/2014JB011184

Key Points:
- Stress drop covaries with recurrence
- Recurrence shows aspects of both time and slip predictability
- Stress drop correlates strongly with the previous stress drop, reflecting an earthquake cycle-long memory

Correspondence to:
N. M. Beeler,
nbeeler@usgs.gov

Citation:
Beeler, N. M., T. Tullis, J. Junger, B. Kilgore, and D. Goldsby (2014), Laboratory constraints on models of earthquake recurrence, *J. Geophys. Res. Solid Earth*, *119*, 8770–8791, doi:10.1002/2014JB011184.

Received 9 APR 2014
Accepted 31 OCT 2014
Accepted article online 8 NOV 2014
Published online 17 DEC 2014

Laboratory constraints on models of earthquake recurrence

N. M. Beeler[1], Terry Tullis[2], Jenni Junger[2,3], Brian Kilgore[4], and David Goldsby[2,5]

[1]Cascades Observatory, U.S. Geological Survey, Vancouver, Washington, USA, [2]Department of Geological Sciences, Brown University, Providence, Rhode Island, USA, [3]Now at BHP Billiton, Houston, Texas, [4]Earthquake Science Center, U.S. Geological Survey, Menlo Park, California, USA, [5]Now at Department of Earth and Environmental Science, University of Pennsylvania, USA

Abstract In this study, rock friction "stick-slip" experiments are used to develop constraints on models of earthquake recurrence. Constant rate loading of bare rock surfaces in high-quality experiments produces stick-slip recurrence that is periodic at least to second order. When the loading rate is varied, recurrence is approximately inversely proportional to loading rate. These laboratory events initiate due to a slip-rate-dependent process that also determines the size of the stress drop and, as a consequence, stress drop varies weakly but systematically with loading rate. This is especially evident in experiments where the loading rate is changed by orders of magnitude, as is thought to be the loading condition of naturally occurring, small repeating earthquakes driven by afterslip, or low-frequency earthquakes loaded by episodic slip. The experimentally observed stress drops are well described by a logarithmic dependence on recurrence interval that can be cast as a nonlinear slip predictable model. The fault's rate dependence of strength is the key physical parameter. Additionally, even at constant loading rate the most reproducible laboratory recurrence is not exactly periodic, unlike existing friction recurrence models. We present example laboratory catalogs that document the variance and show that in large catalogs, even at constant loading rate, stress drop and recurrence covary systematically. The origin of this covariance is largely consistent with variability of the dependence of fault strength on slip rate. Laboratory catalogs show aspects of both slip and time predictability, and successive stress drops are strongly correlated indicating a "memory" of prior slip history that extends over at least one recurrence cycle.

1. Introduction

For large earthquakes, per event displacement and dated recurrence from paleoseismic studies show that recurrence is quasiperiodic [*Schwartz and Coppersmith*, 1984]. Similarly, stress drops and recurrence times from some instrumented intermediate and small earthquakes are highly regular [*Ellsworth*, 1995; *Nadeau and Johnson*, 1998]. The spatial extent of a recurring source is thought to be determined and maintained over time by material and rheological contrasts [*Nadeau and Johnson*, 1998] or geometric boundaries [*Schwartz and Coppersmith*, 1984]. Thus approximately the same fault area fails in repeated events with approximately the same moment, deemed a "characteristic" earthquake by *Schwartz et al.* [1981], and with regularity relatable to the rate of loading [*Wallace*, 1970; *Schaff et al.*, 1999]. To what degree such recurring events are representative of seismicity generally, and to what degree large and hazardous events are characteristic, remains poorly known and controversial [*Wesnousky*, 1994, 1996; *Page et al.*, 2011]. Nonetheless, characteristic recurrence models underlie most regional and national hazards assessments of plate boundaries [*Field et al.*, 2008; *Petersen et al.*, 2008].

For a sequence of recurring earthquakes the average recurrence interval $\bar{t}_r$ is the ratio of the average earthquake slip $\bar{\delta}$ to the loading rate

$$\bar{t}_r = \frac{\bar{\delta}}{\overline{V}_L - \overline{V}_c}, \tag{1a}$$

[*Wallace*, 1970], where the loading rate is the average rate of elastic loading displacement $\overline{V}_L$, minus any rate of fault creep $\overline{V}_c$ that occurs at the source (e.g., precursory or afterslip). For large earthquakes, $\overline{V}_L$ is usually the rate of plate motion. It has been suggested that models of recurrence that account for the fault's physical properties might allow for meaningful predictions of recurrence [e.g., *Bufe et al.*, 1977; *Shimazaki and Nakata*, 1980]. In that case Wallace's definition of recurrence can be equivalently expressed in terms of the fault's failure criteria and frictional sliding properties. For example, the average slip $\bar{\delta}$ is related to the average earthquake stress drop $\overline{\Delta\tau}$ via

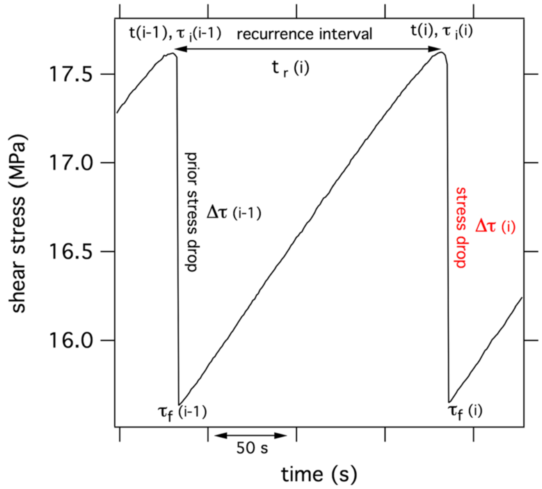

Figure 1. Portion of a laboratory "stick-slip" experiment from the Brown University rotary shear apparatus (experiment fr116cq, see Figure 4 also). The time series of shear stress shows stress drop and recurrence interval as defined throughout this study. The recurrence interval $t_r(i)$ is the time between the initial (peak) stress τ_i $(i-1)$ and τ_i (i) of consecutive failures, $t(i) - t(i-1)$. The initial stress τ_i (i) and final stress τ_f (i) define stress drop $\Delta\tau(i)$, the prior initial and final stresses define the prior stress drop $\Delta\tau(i-1)$.

the elastic stiffness, $\bar{\delta} = \overline{\Delta\tau}/k$, while stress drop is the difference between the initial τ_i and the final stress τ_f (Figure 1), and average recurrence is

$$\bar{t}_r = \frac{\bar{\tau}_i - \bar{\tau}_f}{k(\bar{V}_L - \bar{V}_c)}. \tag{1b}$$

Because geologic and seismologic studies find significant variance in recurrence and in slip or stress drop [e.g., *Schwartz and Coppersmith*, 1984; *Nadeau and Johnson*, 1998], in any formal forecast or hazard analysis, recurrence is represented by a probabilistic expression. Throughout this paper, to characterize the variability of recurrence, stress drop, and initial and final stress, we use the fractional variation (coefficient of variation), the ratio of the standard deviation to the mean, $\sigma_y/\bar{y}$. Here and throughout σ_y is standard deviation of the measured quantity y, for example, σ_{t_r} is the standard deviation of the recurrence interval. In discussing the size of this uncertainty in general terms we often refer to its order; for example, second-order variability is a value of $\sigma_y/\bar{y}$ on the order of 0.1 or 10%, third order is $\sigma_y/\bar{y}$ on the order of 0.01 or 1%, and so on.

For recurring earthquakes of magnitude $M \geq 5$, $\sigma_{t_r}/\overline{t_r}$ is second order or larger, with a representative value of around 0.5 [*Hecker et al.,* 2013]. Therefore, even knowing the location and size of an impending earthquake, and the time and slip of its prior occurrences, there is considerable uncertainty in the time of the next event in the sequence. In previous studies, to generate a predictive model of recurrence, the number of independent variables in equations (1a) and (1b) is reduced to a more manageable number such as 1 [*Bufe et al.,* 1977] or 0 [*Rubinstein et al.,* 2012a], based on physical intuition or a particular hypothesis. For example in the time-predictable model of *Bufe et al.* [1977] creep velocity is assumed to be zero, while the elastic loading rate and initial stress are assumed constant. The physical motivation for these choices is a laboratory-based model in which the onset of slip occurs approximately at a threshold stress. Throughout this report we use the subscript i to denote the event number within the sequence (Figure 1). For the time-predictable model, the previous event's final stress $\tau_f(i-1)$, or equivalently the prior stress drop, $\Delta\tau(i-1)$, directly determines the subsequent recurrence interval $t_r(i)$

$$t_r(i) = \frac{\Delta\tau(i-1)}{kV_L}. \tag{2a}$$

Variability in recurrence is due to variability in the stress drop or more exactly due to variance in the prior final stress $\tau_f(i-1)$. Similarly for the slip-predictable model of *Shimazaki and Nakata* [1980], the same assumptions about creep and loading rate are made and the final stress is assumed constant so that the pending stress drop (slip) is proportional to the recurrence interval,

$$\Delta\tau(i) = t_r(i)kV_L. \tag{2b}$$

To date, arguments about whether models such as equations (2a) and (2b) provide any predictive value for natural recurrence are subjective [*Bufe et al.,* 1977; *Shimazaki and Nakata*, 1980; *Rubinstein et al.,* 2012a]; indeed, *Rubinstein et al.* [2012a, 2012b] have proposed that the next recurrence time $t_r(i)$ is better predicted by using $\bar{t}_r$ over the previous events ($N = 1$, $i-1$) rather than equation (2a) above.

In the current study we present new observations that may inform models of earthquake recurrence. Seismic data do not record absolute levels of initial and final stress, making it difficult to directly confirm the assumptions of models such as equations (2a) and (2b). Furthermore, while geodetic observations indicate effectively constant rates of plate motion, the contribution of creep for many natural earthquake sequences is

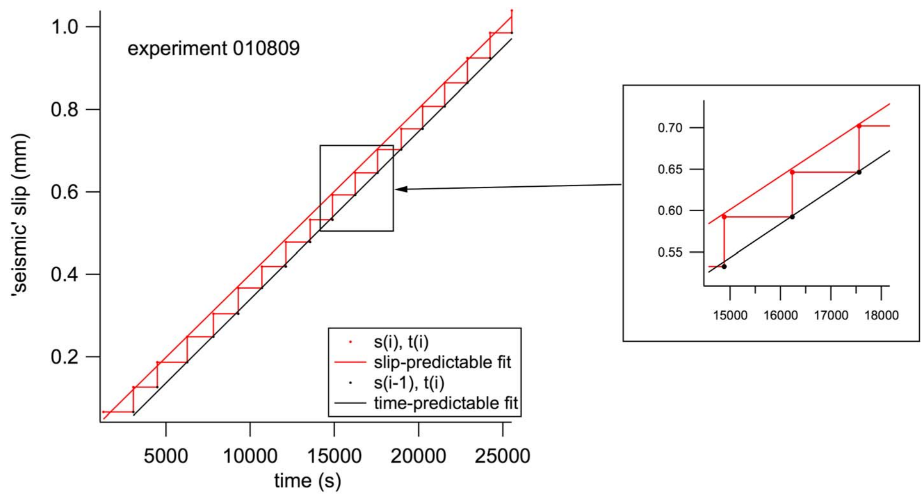

Figure 2. Cumulative slip versus time for the experiment 010809 [*Kilgore and Beeler*, 2010; *Rubinstein et al.,* 2012b]. Slip is calculated from the frictional stress drop data by multiplying by the unloading stiffness (3.3 MPa/mm) and the normal stress (4 MPa). Fits of the data to slip (red) and time predictable (black) models are also shown. See text for a complete description.

difficult to quantify and the nature of loading for small recurring earthquakes is thought to be due to creep of the surrounding fault rather than directly from tectonic loading [*Bufe et al.,* 1977; *Nadeau and Johnson*, 1998]. For these reasons we focus on recurrence in event catalogs generated during laboratory rock friction experiments [*Brace and Byerlee*, 1966]. Primary advantages to laboratory tests are that loading rate is controlled, fault area is constant, and fault slip and stress are measured directly. Thus, while equations (1a) and (1b) suggest that there may be uncertainties associated with up to six variables (t_r, k, V_L, V_c, τ_i, and τ_f), in the lab for a fault with fixed area (fixed stiffness) and controlled loading velocity, the four remaining variables are directly measured. The approach is intended to give more insight into potential covariances among these quantities and should allow for a model of recurrence based on some physical understanding of the fault's shear resistance. In addition, it may be that recurrence in experiments shares some similarity in process with small shallow or with larger earthquakes and that the controlled circumstances of the laboratory can reveal systematic predictability that may be applied to better understand natural recurrence. An advantage of the rotary shear geometry used in the present study is that it provides essentially unlimited sliding displacement. At short displacement, stress drop, recurrence intervals, and other frictional properties evolve significantly with time or slip. This complicates the analysis of data from such tests because models like equations (2a) and (2b) are usually interpreted as requiring fault properties to be constant (stationary) [*Rubinstein et al.,* 2012a, 2012b]. To deal with displacement or time dependencies of fault properties in experimental catalogs *Rubinstein et al.* [2012b] developed approaches to remove the trends. In the experiments in this paper the fault surfaces are slid until such time, and displacement dependencies are no longer apparent [*Beeler et al.,* 1996].

1.1. Laboratory Earthquake Recurrence

Following *Brace and Byerlee* [1966], laboratory-scale recurrence experiments are often referred to as undergoing "stick-slip". In such a test (Figure 1), the fault is loaded at a constant rate intended to simulate tectonic loading. The fault remains apparently stuck for some period of time, analogous to a natural earthquake recurrence interval, and then fails, slipping rapidly producing a stress drop through unloading of elastic strain stored in the rock and testing machine. The sequence repeats, resulting in a catalog of events whose statistical properties can be studied and compared to natural sequences and to existing earthquake recurrence models or used to develop new models of recurrence.

As an example of a laboratory sequence, and for consistency with previous work, Figure 2 shows the time series of slip from a catalog [*Kilgore and Beeler*, 2010] used in a recent recurrence study [*Rubinstein et al.,* 2012b]. This particular example is used here because it is the only experiment analyzed by *Rubinstein et al.* [2012b] that had no coherent slip- or time-dependent trend in stress drop or recurrence. As the same is true of all of the new experiments described later in this paper, we assume throughout that the fault properties are stationary. In the following brief analysis of this example we show some of the characteristics of lab catalogs and how they compare with predictions of the recurrence models, equations (2a) and (2b).

The experiment, run 010809, follows the approach of *Junger et al.* [2004] and was conducted on a large biaxial press at the U.S. Geological Survey (USGS) in Menlo Park, California [*Dieterich*, 1981]. The press accommodates samples 1.5 × 1.5 × 0.4 m in dimension with a precut fault surface along the diagonal, 45° to the long dimensions, resulting in a fault surface of length and depth of 2 and 0.4 m, respectively. The load-bearing elements are seven steel plates stacked and bolted together. The fault is loaded along the outward faces of the 1.5 m long sides of the fault blocks using four flat jacks pressurized with hydraulic oil using a computer-controlled servo system. Flat jacks on opposite sides of the blocks are pressurized equally, thus, there are two orthogonal-controlled forces applied to the blocks. Teflon plates between the frame and the jacks permit free slip at this interface. Similarly, the weight of each of the sample halves are supported below by three stationary jacks which have Teflon-surfaced load-bearing plates to permit easy horizontal motion of the blocks in response to the loading stresses provided by the flat jacks. Samples are Sierra White granite from Raymond, California. The fault surface was roughened using a specially designed frame and 30 grit SiC as described by *Okubo and Dieterich* [1984]. The average shear and normal stress on the fault are derived from transducers recording the pressure in the two independent sets of flat jacks. These two pressures are assumed to be the principal stresses σ_1 and σ_3. The sequence of failure events was conducted at a normal stress of 4 MPa. The fault was loaded by raising the shear stress at 0.0001 MPa/s while holding the normal stress constant until an unstable shear failure of the fault occurred. Rapidly accelerating slip detected by an accelerometer triggers closure of hydraulic valves isolating the flat jacks from the servo control system to prevent a response to the sudden changes in the shear and normal stress. To repeat the experiment, the servo system is reset, the hydraulic isolation valves are opened, and the loading procedure is repeated. The time required to reset the servo system is small compared to the average recurrence interval. The static shear stress drop was calculated from the flat jack pressures, and the duration of loading to failure is reported as the recurrence interval.

Ideally, the servo control system would maintain static pressure in the loading jacks during the event; unfortunately, the triggered valve closure is relatively slow, occurring in approximately 0.4 s. Fortunately, the response time of the servo system is slow relative to the duration of the dynamic rupture which is roughly 2 ms. The servo system responds to stress changes in around 0.01 s, which is also the sampling rate of the data acquisition system. While the measurements of the failure stress are well resolved, the values of the final stress may be somewhat influenced by loading from the servo-controlled loading system prior to valve closure. Additional details of the loading in similar experiments are found in *Beeler et al.* [2012]. The contributions of the loading system to the final stress values can be estimated from the measured rate that the servo control system raises the shear stress prior to value closure (~0.125 MPa/s, see *Beeler et al.* [2012, Figure A2]) and the sampling interval (0.01 s). Accordingly, the final stress values may be underestimated by up to 0.001 MPa. Since this is a systematic bias to slightly larger values, it should not affect the conclusions of our analysis. The standard deviation of the final stress (0.002 MPa) is of the same order as that for the failure stress (Table 1), suggesting that there are no significant machine effects on the variability.

For run 010809, variability in static stress drop and recurrence interval are modest with fractional uncertainties of 8 and 11%, respectively (Table 1). Stress drop is defined by the initial and final stresses (Figure 1); these have uncertainties of less than 1%, much smaller than that of the stress drop. The higher variability of the stress drop arises because it is a relatively small fraction of the ambient stress, roughly 10% of the initial stress. The relation between slip and recurrence is shown graphically by the standard "stair step" construction (Figure 2). Here the stress drop data are converted to slip using the unloading stiffness and then plotted in sequence in absolute time, *t*, assuming that there is no interseismic slip. Plots of this type were used in the development of the physically motivated recurrence models (2a) and (2b) [*Bufe et al.*, 1977; *Shimazaki and Nakata*, 1980]. The failure times $t(i)$ and the cumulative coseismic slip values $\delta(i)$ (red points) can be compared with the slip-predictable model. The previous event slip values $\delta(i-1)$ and subsequent failure times $t(i)$ (black points) can be compared to the time-predictable model of *Bufe et al.* [1977]. Fits to the cumulative slip and time data with either model are very good. The coefficient of determination (R^2) ($R^2 = 1 - \frac{\sum_{i=1}^{N}(y(i)-f(i))^2}{\sum_{i=1}^{N}(y(i)-\bar{y})^2}$ where y(i) are data, f(i) are model predictions, and $\bar{y}$ is the data mean. R^2 is a measure of the predictive power of a linear model.) exceeds 0.999 for both the time- and slip-predictable models fit to the data in this way. Based on these observations, to second order, this laboratory data set is periodic and therefore also both time predictable and slip predictable.

Table 1. Experiment 010809 (USGS)[a]

t_{start} (s)	t_i (s)	τ_i (MPa)	τ_f (MPa)	$\Delta\tau$ (MPa)	t_r (s)
10,605.00	11,877.16	2.968	2.742	0.218	1,272.16
11,952.74	13,738.98	2.964	2.765	0.199	1,786.22
13,876.16	15,285.26	2.975	2.772	0.203	1,409.06
15,549.84	17,325.02	2.958	2.756	0.203	1,775.12
17,406.68	18,961.32	2.963	2.779	0.184	1,554.56
19,096.92	20,590.18	2.969	2.762	0.207	1,493.81
20,675.94	22,063.26	2.957	2.785	0.172	1,387.26
22,223.28	23,646.16	2.966	2.773	0.193	1,422.84
23,844.74	25,291.92	2.954	2.774	0.180	1,447.12
25,385.72	26,713.68	2.975	2.777	0.198	1,327.9
26,829.72	28,184.26	2.971	2.794	0.177	1,354.44
28,282.56	29,610.14	2.980	2.795	0.185	1,327.52
29,712.32	31,121.68	2.970	2.803	0.168	1,409.26
31,310.44	32582.68	2.969	2.804	0.165	1,272.16
32,677.84	33978.94	2.990	2.803	0.188	1,300.98
34,071.00	35424.02	2.991	2.794	0.198	1,352.96
36,006.72	37352.12	2.995	2.794	0.202	1,345.32
	Mean	2.9725	2.7822	0.1900	1,418.3
	Std	±0.012	±0.019	±0.015	±151.81
	Cv	(0.004)	(0.007)	(0.077)	(0.107)

[a]Parameters: t_{start} = starting time of the loading cycle (USGS) in s; t_i = initial time, time of the "initial stress" in s; τ_i = initial stress in MPa; τ_f = final stress in MPa; $\Delta\tau$ = static stress drop in MPa; t_r = recurrence interval in s; and V_L = loading velocity in μm/s.

However, the models, equations (2a) and (2b), are intended to prospectively predict the next event in the sequence rather than fit the overall sequence retrospectively, as done in the fits shown in Figure 2. In this predictive context, recurrence times and stress drops are not well forecast by either of the models, equations (2a) and (2b), [*Rubinstein et al.,* 2012b]. This is apparent in a plot of the individual stress drops and recurrence intervals (Figure 3). In this diagram, fits to the slip- and time-predictable models are lines defined by two points: the origin (0,0) and the point containing the means $\left(\overline{t_r}\,\overline{\Delta\tau}\right)$. Analyzed in this way, these linear models do not fit this data set well; R^2 is 0.33 and −1.24 for the time- and slip-predictable models, respectively. There are apparently uncorrelated variations in stress drop and recurrence about their mean values.

1.2. Purpose

The purpose of the present study is to characterize laboratory recurrence and to develop a preliminary model of it that may be extrapolated to natural conditions. Because of the relatively small number of recurrences and expected variability in the measurements, it is unlikely that the example data set for experiment 010809 contains enough information to develop a useful physical model of recurrence at constant loading rate that could be extrapolated to natural stresses and stressing rates. Among the issues that need to be addressed are whether recurrence is essentially periodic within small uncertainties at constant loading rate, as might be concluded from Figures 2 and 3, or if there is some correlation between the recurrence interval and stress drop. Also, if there is correlation between recurrence and stress drop, then which is the independent variable? The data from constant loading rate experiments in this study have smaller variability than in previous studies, contain many tens to many hundreds of events, allow better definition of the uncertainties, and provide leverage to the search for possible covariance of stress drop with recurrence that is not resolved in small catalogs (Table 1).

Stressing rate differences between experiments and the Earth also are an important consideration since many small repeating earthquake sequences are driven to failure by creep of the surrounding fault [*Nadeau and Johnson*, 1998]. In cases where the creep rate is variable, for example, during afterslip following a large nearby earthquake [*Schaff et al.,* 1999; *Uchida et al.,* 2004], or deep episodic slip [*Thomas et al.,* 2012], obviously, the loading rate is variable. For nonconstant loading, the recurrence interval is to first order inversely proportional to the loading rate as in equations (2a) and (2b). That is, to produce first-order variations in recurrence interval for a fault that is highly periodic (Figures 2 and 3) requires significant changes in loading rate. Related to large changes in loading rate are expected changes in stress drop; previous

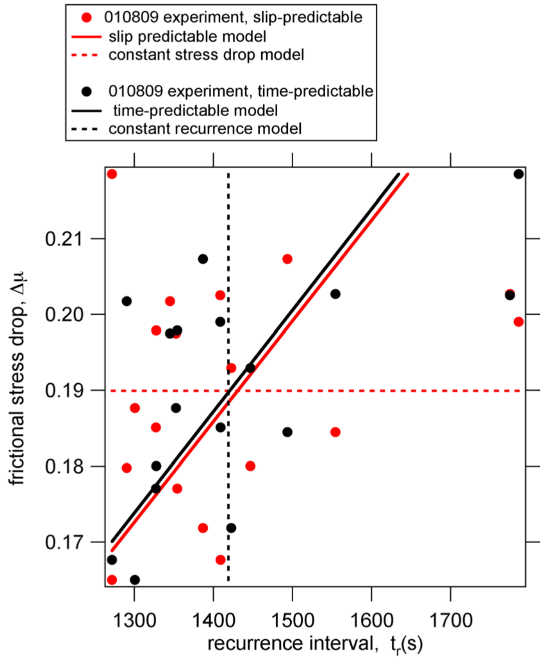

Figure 3. Laboratory earthquake recurrence data after *Junger et al.* [2004] from the USGS large biaxial press [*Dieterich*, 1981]. Data are from the same experiment shown in Figure 2: 17 recurrences plotted as stress drop normalized by normal stress (frictional stress drop) versus recurrence interval. The events are displayed in two different ways. In red symbols are stress drop versus recurrence to enable comparison with a fit of this data with the slip predictable model of *Shimazaki and Nakata* [1980] (red solid line). For reference is a fit of the data using a constant stress drop model (red dashed line). The data are also plotted as recurrence versus previous stress drop (black symbols) to enable comparison with a fit of this data to the time-predictable model of *Bufe et al.* [1977] (black solid line). Note that contrary to the choice of vertical and horizontal axes, for this model, stress drop is the independent variable. For reference is a fit of this data with a constant recurrence interval model (black dashed line). The slip- and time-predictable model fits are nearly the same, as expected. The slight difference results from small differences in the mean stress drop and mean recurrence due to there being 17 data points for the fit to the slip-predictable model and only 16 for the fit to the time-predictable model.

laboratory studies [*Wong and Zhao*, 1990: *Karner and Marone*, 2000; *McLaskey et al.*, 2012] and studies of natural earthquake recurrence [*Scholz et al.*, 1986; *Kanamori and Allen*, 1986; *Vidale et al.*, 1994] find systematic variations in stress drop with recurrence time. The loading rates in the experiments in this study span 4 orders of magnitude.

Issues related to uncertainty extend to the development of physical models, for example, both the time and slip predictable models assume an exactly constant value of the final or failure stress, unrealistic assumptions even in controlled laboratory tests due to measurement and intrinsic uncertainties. Sources of uncertainty such as uncontrolled loading rate, static stress transfer from nearby sources, and material and stress heterogeneity are liable to be more numerous and larger in natural catalogs. Based on the experiments we construct a conceptual model of recurrence that also accounts for expected uncertainties that arise even in carefully prepared and controlled experiments. Among the conclusions is that laboratory recurrence has aspects of both time and slip predictability; these tendencies are coupled and arise directly from the rate-dependent physical processes that lead to repeated failure. In addition, both stress drop and recurrence are found to vary systematically but nonlinearly with loading rate.

2. Experiments

The experiments were conducted at Brown University in a high-pressure rotary shear apparatus [*Tullis and Weeks*, 1986]. Catalogs of recurrence with large event numbers and at varying, controlled loading rates can be routinely acquired using this testing machine where the available displacement is effectively unlimited. The experiments are on initially bare surfaces of Cheshire quartzite (experiments fr102cq and fr116cq) and silica glass (fr97sg). The sample assembly is as described by *Beeler et al.* [1996]. The two cylindrical sample rings are epoxied into hardened steel sample grips. Sample rings were cored from blocks of rock or glass. The rock rings were ground to height with a surface grinder. Surface finish was obtained by grinding with wet #24 “dyanblast” SiC grit on a glass plate, resulting in a centerline average roughness of ~0.01 mm [*Power et al.*, 1988]. The outer diameter of the cylinders is 53.98 mm, the inner diameter is 44.45 mm, the total area of the fault is 735 mm^2, and the centerline circumference is 154.61 mm. The upper sample grip is held fixed, and the lower grip is rotated by a steel piston which also transmits the axial load. Shear and normal stress applied to the sample by the piston are measured with an internal torque/load cell. A sliding, gas-tight jacket of Teflon rings and O rings excludes the confining medium, in this case, nitrogen gas. The Teflon rings remain stationary with respect to the upper and lower sample rings and slide against one another. The upper sample ring is vented to the atmosphere to prevent the buildup of pore pressure in case of a pressure leak around the O rings. The experiments were conducted at room temperature, a constant normal stress of 25 MPa, confining pressure of 21 MPa, and loading rates between 0.01 μm/s and 10 μm/s.

Table 2. Experiment fr116cq (Brown University)

t_i (s)	τ_i (MPa)	τ_f (MPa)	t_r (s)	$\Delta\tau$ (MPa)
847,181.62	17.708	15.75		1.958
847,332.15	17.636	15.721	150.53	1.915
847,475.37	17.641	15.694	143.22	1.947
847,624.83	17.65	15.685	149.46	1.965
847,779.40	17.655	15.659	154.57	1.996
847,931.77	17.652	15.652	152.37	2
848,084.15	17.65	15.646	152.38	2.004
848,236.80	17.635	15.646	152.65	1.989
848,387.24	17.648	15.627	150.44	2.021
848,539.70	17.662	15.632	152.46	2.03
848,697.27	17.662	15.629	157.57	2.033
848,856.83	17.664	15.627	159.56	2.037
849,006.21	17.62	15.631	149.38	1.989
849,161.63	17.63	15.627	155.42	2.003
849,321.27	17.654	15.642	159.64	2.012
849,476.71	17.624	15.632	155.44	1.992
849,630.16	17.619	15.641	153.45	1.978
849,781.87	17.623	15.656	151.71	1.967
849,930.19	17.631	15.659	148.32	1.972
850,081.57	17.642	15.677	151.38	1.965
850,235.01	17.637	15.684	153.44	1.953
850,387.61	17.65	15.654	152.6	1.996
850,530.89	17.598	15.642	143.28	1.956
850,682.26	17.63	15.646	151.37	1.984
850,835.87	17.625	15.626	153.61	1.999
850,986.43	17.606	15.617	150.56	1.989
851,136.81	17.609	15.593	150.38	2.016
851,289.26	17.582	15.594	152.45	1.988
851,437.70	17.576	15.624	148.44	1.952
851,585.96	17.58	15.596	148.26	1.984
851,740.31	17.565	15.597	154.35	1.968
851,897.88	17.579	15.615	157.57	1.964
852,044.06	17.559	15.619	146.18	1.94
852,194.57	17.564	15.581	150.51	1.983
Mean	17.626	15.642	151.91	1.984
Std	±0.034	±0.036	±3.85	±0.028
Cv	(0.002)	(0.002)	(0.025)	(0.014)
$r\ \Delta\tau(i)\ t_r(i)$	0.55			
$r\ \Delta\tau(i-1)\ t_r(i)$	0.96			

3. Observations

In this section the experimental observations are described and analyzed. Experiments at constant loading rate, as in experiment 010809, are considered first immediately below. The measurements made in experiments at different loading rates are described in the second subsection. In both cases, variability and covariability of stress drop and recurrence are defined. Empirical descriptions of the stress drop, recurrence interval, failure stress, final stress, and the variances of these quantities are developed that account for differences in loading rate.

3.1. Constant Loading Rate

During the bare surface quartzite experiment (fr116cq), while sliding at a constant loading rate, $V_L = 0.3162\ \mu$m/s, 34 repeated stick-slip failures were collected at displacements between 101.7 and 103.4 mm (Table 2). The peak strength preceding failure and the minimum stress following the slip event are used to define the stress drop (Figure 1). This data set has two advantages over experiment 010809. First, there are twice as many events and, second, the variability in the initial and final stresses, the stress drop, and the recurrence interval are many times smaller. The higher reproducibility likely arises because of the relatively large displacements attained before making the measurements and the use of a controlled constant displacement rate-loading system. The standard deviation of the initial stress and final stress are 0.2% of their means, while deviations in the stress drop and recurrence interval are a few percent at most. These improvements allow better

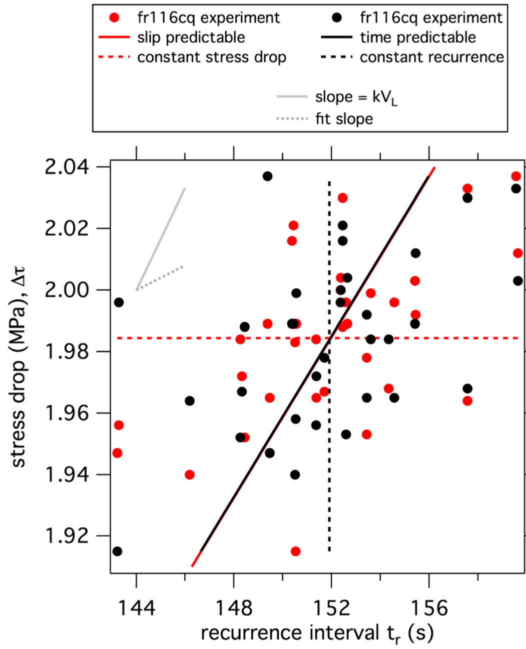

Figure 4. Thirty-four recurrences from sliding on initially bare surfaces of quartzite (fr116cq) in the Brown University rotary shear apparatus [*Tullis and Weeks*, 1986]. The data are plotted as stress drop versus recurrence (red) and as recurrence versus previous stress drop (black symbols). The black and red reference lines are shown are as in Figure 3 (see Figure 3 caption). An additional reference line in grey has a slope that is the stressing rate, the product of the machine stiffness and the loading rate. For comparison is the slope of a linear fit to the stress drop versus recurrence shown as the dashed grey line. The data show covariance of stress drop with recurrence regardless of whether the stress drop or previous stress drop are considered (see text and Table 2).

definition of the relations between stress drop and recurrence. These data are plotted in Figure 4 as stress drop versus recurrence and as previous stress drop versus recurrence, in the same way as for experiment 010809 in Figure 3. The time- ($N=33$) and slip-predictable ($N=34$) models shown for reference are essentially identical (red and black solid lines), as expected when the number of events is large and the variances are low. Furthermore, stress drop covaries with recurrence. The standard linear covariance (r) ($r=\dfrac{\sum_{i=1}^{N}(x(i)-\bar{x})(y(i)-\bar{y})}{\sqrt{\sum_{i=1}^{N}(x(i)-\bar{x})^2(y(i)-\bar{y})^2}}$) between $\Delta\tau(i)$ and $t_r(i)$ (black symbols) (Figure 4) is 0.55 (Table 2); based on standard estimates of the probability [*Taylor*, 1997], there is a 0.08% chance that uncorrelated data would produce a correlation coefficient this high or higher. The standard linear covariance between the prior stress drop $\Delta\tau(i-1)$ and $t_r(i)$ (red) (Figure 4) is 0.46; there is 0.07% chance that uncorrelated data would produce a correlation coefficient this high or higher.

The trend between stress drop $\Delta\tau(i)$ and recurrence $t_r(i)$ in this data set (Figure 4) is shown as the dashed grey line offset from the data for clarity. This trend differs in slope and physical origin from a strong relationship between stress drop and recurrence found by *Karner and Marone* [2000] using the double direct shear geometry, which they denoted β_2. At a single loading rate, both stress drop and recurrence interval vary systematically in *Karner and Marone* [2000]. For laboratory-measured stick-slip, where all of the slip occurs seismically ("true" stick-slip), if the range of stress drops is wide, to first order, the recurrence interval and stress drop will follow equations (2a) and (2b) with proportionality determined by the imposed rate and elastic properties of the loading system [*Beeler et al.*, 1998] as *Karner and Marone* [2000] found; their value is $\beta_2=kV_L$. This is the original physical motivation for the time-predictable and slip-predictable models. For fr116cq the trend (Figure 4, dashed grey line) is lower than that predicted by the loading velocity and stiffness, kV_L = 0.017 MPa/s (Figure 4, solid grey line).

For the experiment on bare surfaces of silica glass (fr97sg), two constant loading rate data sets, at $V_L=1$ μm/s and 10 μm/s, were collected at displacements between 13 and 92 mm, consisting of 1947 repeated failures (Table 2). The loading rate was cycled between 1 and 10 μm/s at every 1 mm of load point displacement (Figure 5a) so these are discontinuous, constant loading rate catalogs. Again, the peak strength associated with failure and the minimum stress following stress drop are used to define the stress drop. In comparison to fr116cq, the standard deviations in the initial stress (peak stress) and final stress are larger than in that continuous loading rate experiment, up to 1.3% of the mean. However, the deviations in stress drop and recurrence interval are only slightly higher than that in fr116cq and are a few percent. The data acquisition rate limits the resolution of recurrence interval, resulting in the "binned" nature of the recurrence data (Figures 5b and 5c). The acquisition rate in Figure 5b is ~1 Hz, resulting in a limit on the resolution of recurrence of about 1 s. The corresponding rate in Figure 5c is ~10 Hz and the resolution limit is 0.1 s. This undersampling produces possible errors on the failure and final stresses. In both cases the stressing rate times the sampling rate is 0.05 MPa. However, there is precursory slip so at the peak stress the effective

10.1002/2014JB011184

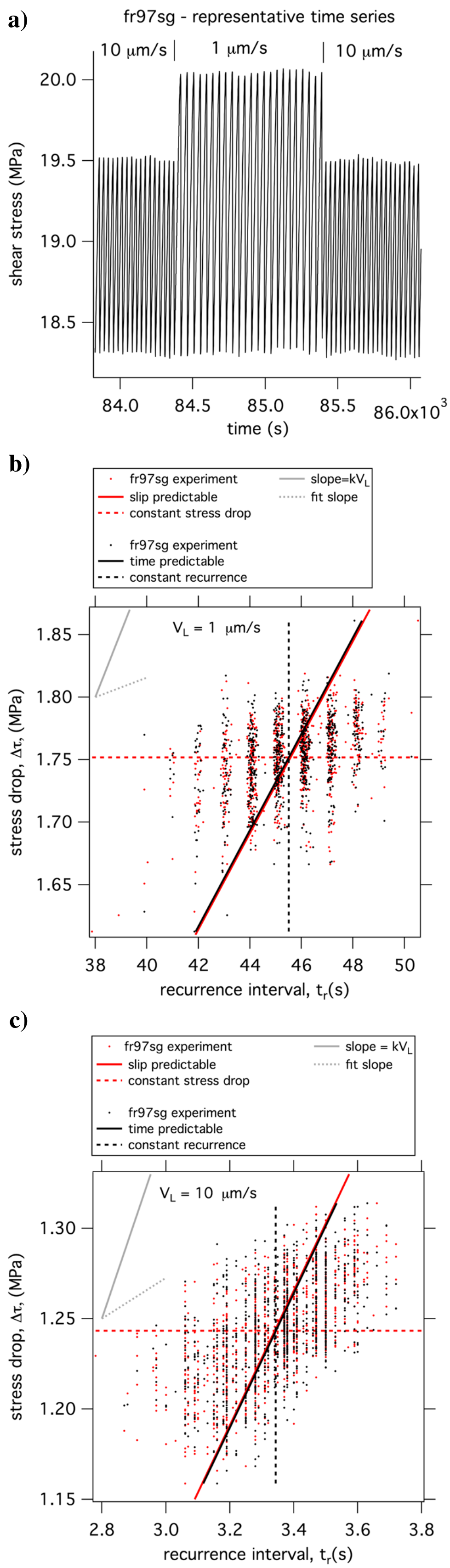

stressing rate is zero and the peak is always well resolved (see Figure 1). The final stress has the same resolution constraint, and there is much less afterslip than precursory slip so the final stress has a measurement error of up to 0.05 MPa, which is 3 to 4% of the average stress drop. Although these are small measurement errors, they are systematically related to the measurement error on the recurrence. Thus, if the data were perfectly periodic, the measured recurrence and stress drop would fall on a line that has a slope of the stressing rate kV_L with the maximum values being near the actual recurrence and stress drop and the minimum values being the actual values minus the maximum errors. In other words, the data would fall on the *Karner and Marone* [2000] β_2 line.

Despite these complications of sampling rate, again, stress drop covaries with recurrence. Comparing the stressing rate (grey solid lines in Figures 5b and 5c) to the trend, from a linear fit to the data (grey dash line), shows that the measurement error does not determine the covariance between stress drop and recurrence. The standard linear covariance between $\Delta\tau(i)$ and $t_r(i)$ (black) (Figures 5b and 5c) is 0.47 to 0.64 (Table 3); because of the large catalog size, it is extremely unlikely for uncorrelated data to have a correlation coefficient this high or higher ($<1 \times 10^{-46}$% chance). The covariance between the prior stress drop $\Delta\tau(i-1)$ and recurrence $t_r(i)$ (black) (Figures 5b and 5c) is between 0.34 and 0.57, and it is highly unlikely for uncorrelated data to result in a correlation coefficient this high or higher ($<1 \times 10^{-21}$% chance).

Because stress drop is the difference between the failure and final stress, it is the individual covariances of these stresses and recurrence that are more fundamental to understanding relations between stress

Figure 5. Recurrence from sliding on initially bare surfaces of silica glass (fr97cq) in the Brown University rotary shear apparatus [*Tullis and Weeks*, 1986] at loading rates of V_L = 1 μm/s (N = 859), and V_L = 10 μm/s (N = 1096). (a) Representative shear stress time series showing the discontinuous nature of the catalogs consisting of multiple sequences at loading of 1 and 10 mm/s. (b and c) The data are plotted as stress drop versus recurrence (red symbols) and as recurrence versus previous stress drop (black symbols). The reference lines shown are as in Figures 3 and 4 (see Figure 3 and 4 captions). The data show covariance of stress drop with recurrence regardless of whether the stress drop or previous stress drop are considered. The data acquisition rate limits the resolution of recurrence interval, resulting in the "binned" nature of the recurrence data. The acquisition rate in Figure 5b was ~1 Hz, resulting in a limit on the resolution of recurrence of about 1 s. In Figure 5c the rate was ~10 Hz and the resolution limit is 0.1 s.

Table 3. Experiment fr97sg (Brown University)

	τ_i (MPa)	τ_f (MPa)	t_r (s)	$\Delta\tau$ (MPa)
		V_L = 1 μm/s, N = 859		
Mean	20.33	18.58	45.52	1.75
Std	±0.25	±0.25	±1.79	±0.030
Cv	(0.012)	(0.013)	(0.039)	(0.017)
$r\ \Delta\tau(i)\ t_r(i)$	0.47			
$r\ \Delta\tau(i-1)\ t_r(i)$	0.34			
		V_L = 10 μm/s, N = 1096		
Mean	19.83	18.58	3.34	1.24
Std	±0.27	±0.25	±0.16	±0.028
Cv	(0.014)	(0.014)	(0.047)	(0.022)
$r\ \Delta\tau(i)\ t_r(i)$	0.64			
$r\ \Delta\tau(i-1)\ t_r(i)$	0.57			

drop and recurrence. Furthermore, it is one or the other of the failure or final stress that vary with recurrence in the slip- and time-predictable models. To examine the relationships among these stresses and recurrence we use the highest resolution data set. For the experiment fr116cq, the uncertainties on the stresses are nearly an order of magnitude smaller than for experiment 010809 and for fr97sg. For fr116cq, the failure stress increases with increasing recurrence (Figure 6a and 6b, upper traces), whereas the final stress decreases with increasing recurrence (Figure 6a and 6b, lower traces). The lines are fits to the data. These trends appear regardless of whether the stresses considered are those following a recurrence interval or those preceding the recurrence interval, although the trends are stronger and are only statistically different from zero for the stresses following the recurrence (see caption to Figure 6). So unlike the slip- and time-predictable models, neither the failure nor final stresses are strictly constant in this data set. On the other hand, like the slip- and time-predictable models, the failure and final stresses correlate with recurrence, the primary difference being that both stresses correlate, rather than just one.

In the absence of physical models, it is difficult to understand the relations between stress drop and recurrence or absolute stress and recurrence in these data sets. For example, because recurrence correlates with prior stress drop and subsequent stress drop correlates with recurrence, it is unclear which is the dependent variable; this becomes, perhaps, even less clear when the failure and final stresses are considered. It is also difficult to think about these data in the context of existing time- and slip-predictable models because the data sets show aspects of both models and because the models, as originally defined, are mutually exclusive. The observations instead suggest a physical model in which the independent variable is some other fault property that influences stress drop and recurrence, a property that more naturally explains their interdependence as an apparent effect rather than as cause and effect.

3.2. Variable Loading Rate

A necessary approach to establishing relations between stress drop and recurrence is to vary these quantities more significantly than in the experiments shown thus far, where the deviations are only a few percent. Physical models with elastic rebound suggest that recurrence should vary approximately inversely with loading rate [*Beeler et al.,* 1998, 2001], and there are examples of stick-slip at different loading rates in the rock and analog fault friction literature, notably, *Wong and Zhao* [1990], *Karner and Marone* [2000], and *McLaskey et al.* [2012]. The relation of stress drop to recurrence is in some cases not explicitly defined, but it is empirically well described by *Karner and Marone* [2000] where it conforms to the expectation. However, at constant loading rate, stress drop and recurrence vary significantly in *Karner and Marone* [2000] relative to the most highly variable data set considered so far, experiment 010809, so we analyze the higher resolution results from earlier experiments [*Weeks et al.,* 1991] instead. The essential aspects of recurrence, consistent with the previous studies, are apparent by superimposing the $V_L = 1$ and 10 μm/s data sets from fr97sg (Figure 5a and 5b) on the same plot (Figure 7a and 7b). Recurrence changes by approximately an order of magnitude for a 10 times change in loading rate. Meanwhile, the stress drop changes about 10%, increasing with decreasing loading rate, consistent with previous laboratory and modeling studies of rock friction [e.g., *Karner and Marone*, 2000; *He et al.,* 2003; *McLaskey et al.,* 2012]. The reference lines in Figure 7a indicate that strict constant recurrence or constant stress drop is not adequate for these data. A physical model where both stress drop and recurrence interval vary with loading velocity (the control variable in the experiments) is required. This is consistent with the rock friction literature wherein it is thought, on the basis of numerical simulations, that the "steady state rate dependence" of the fault strength, $d\tau_{ss}/d\ln V = -\sigma_n(b-a)$, [*Dieterich*, 1979; *Ruina*, 1983] controls both quantities [e.g., *Beeler et al.,* 2001]. Furthermore, the covariance of stress drop with recurrence at each loading rate is

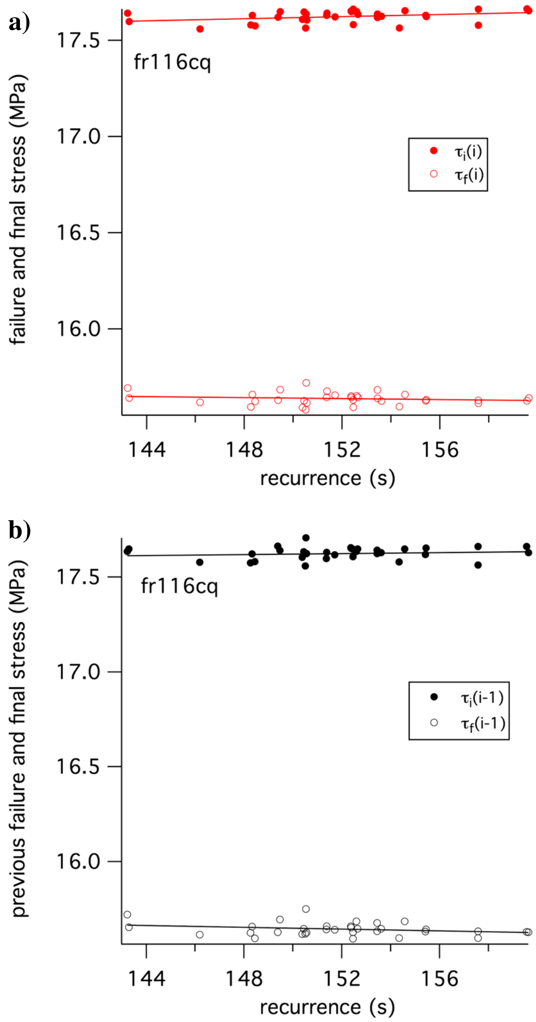

Figure 6. Variation of initial and final stresses with recurrence in quartzite experiment fr116cq. (a) Failure and final stresses defining the stress drop $\Delta\tau(i)$ following recurrence interval $t_r(i)$. The lines are fits to the data. Both show shallow slopes: an increase in the initial strength with recurrence and a decrease in final stress with recurrence. These trends have nonzero slopes; for $\tau_i(i)$ the slope is 0.0027 MPa/s ± 0.0014 and for $\tau_f(i)$ the slope is −0.0024 MPa/s ± 0.0016. (b) Initial and final stresses defining the stress drop $\Delta\tau(i-1)$ preceding the recurrence interval $t_r(i)$. The lines are fits to the data. As in Figure 6a, both stresses show weak correlation with recurrence interval: an increase in the initial strength with recurrence and a decrease in final stress with recurrence. However, these trends are not as strong as in Figure 6a and within the uncertainty are not significantly different than zero: for $\tau_i\,(i-1)$ the slope is 0.0013 MPa/s ± 0.0014 and for $\tau_f\,(i-1)$ the slope is −0.0013 MPa/s ± 0.0014.

different, with $d\Delta\tau/dt_r$ increasing with increasing loading velocity, suggesting that this covariance is also due to the rate dependence of fault strength.

A separate data set from silica glass experiment fr97sg (Table 4) shows the same kind of behavior. The data are from sliding at loading rates between 10 and 0.1 μm/s, at load point displacements between 91.5 and 97.4 mm. Between 91.5 and 93.4 mm displacement, a sequence of loading rate steps from 10 to 1, to 0.316 and to 0.1 μm/s produced recurring events (Table 4); at lower loading velocities of 0.0316, 0.01, and 0.0032 μm/s, slip was stable. When the loading rate was increased in a stepwise fashion, eventually back to 0.1 μm/s at a load point displacement of 95.2 mm, the fault began to again undergo near-periodic slip that continued at loading rates of 0.316, 1, 10, and 1 μm/s again (Table 4) out to a load point displacement of 97.4 mm. This is thus a catalog with four different constant loading rates, but the data at each loading rate are not continuous. These data define a similar relation between stress drop and recurrence (Figure 7b) as in the larger catalogs (Figure 7a). An analogous data set for quartzite (fr102cq) at load point displacements between 92.5 and 93.4 mm also shows a systematic relationship between stress drop and recurrence (Figure 7c). These were collected at loading rates of 0.316, 0.1, 0.0316, and 0.01 μm/s. Empirically the relationship between stress drop and recurrence is nonlinear and is consistent with the previous experimental work on room temperature behavior of rock and analog material friction [*Wong and Zhao*, 1990; *Karner and Marone*, 2000; *McLaskey et al.*, 2012] which show a logarithmic dependence (Figure 7a) of the form

$$\Delta\tau = c\ln\frac{t_r}{t_0}, \tag{3}$$

where t_0 is the intercept, the projected recurrence interval at zero stress drop, and c ln (10) is the slope in a semilog plot (Figure 8a). Because of the large differences in loading velocity, the fit to the recurrence $t_r(i)$ and stress drop $\Delta\tau(i)$ shown in Figure 7 is essentially identical to a fit to this catalog that results if the prior stress drop $\Delta\tau(i-1)$ is used instead.

3.3. Normalized Stress Drop and Recurrence

An aspect of these laboratory recurrence data that deviates markedly from physical models such as *Bufe et al.* [1977] and *Shimazaki and Nakata* [1980] and most other conceptual descriptions of recurring earthquakes is that the experiments show significant interevent slip (precursory and afterslip) [*Wallace*, 1970]. Qualitatively, the amount of interevent slip in these catalogs can be determined by normalizing the stress drop by the normal stress ($\Delta\tau/\sigma_n$) and normalizing the recurrence using the fault stiffness, k, normal stress, σ_n, and the loading velocity ($t_r V_L k/\sigma_n$) (Figure 8b). Occurrences with no interevent slip ("true" stick-slip) plot on the

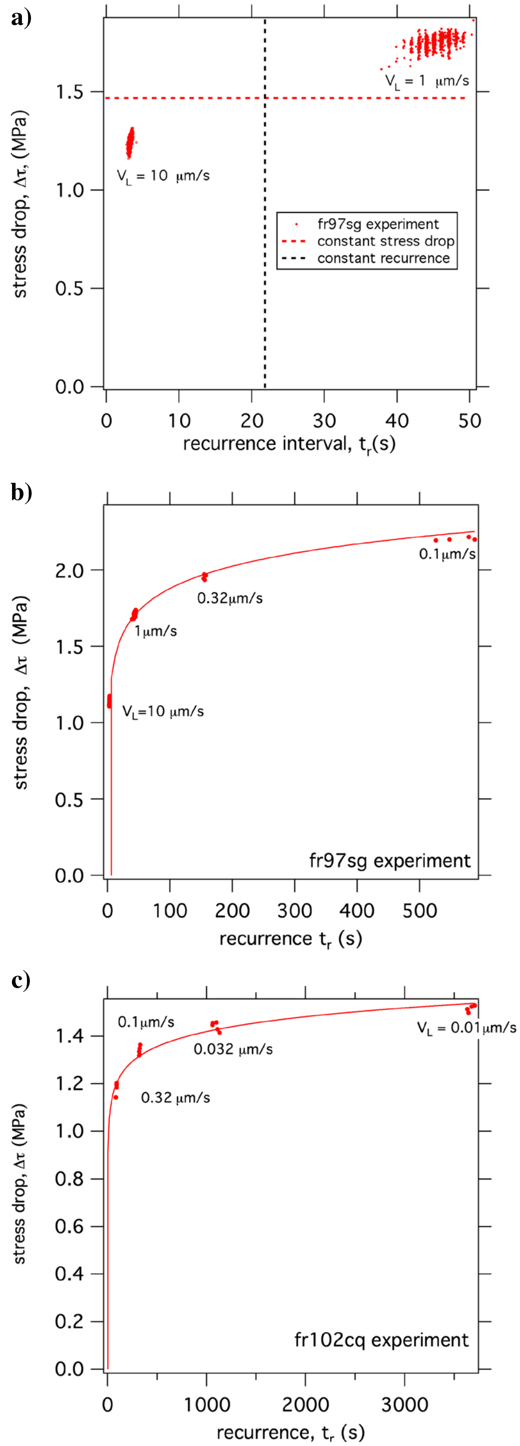

Figure 7. Recurrence from sliding on initially bare surfaces of silica glass (fr97sg) and quartzite (fr102cq) in the Brown University rotary shear apparatus [*Tullis and Weeks*, 1986] at loading rates between 0.032 and 10 µms. (a) fr97sg at $V_L = 1$ and $V_L = 10$ µm/s. These are the same data shown in Figures 5a and 5b. Reference lines are constant stress drop (red dashed) and constant recurrence (black dashed) as defined by the means. (b) fr97sg at $V_L = 10$, 1, 0.32 and 0.1 µm/s. The solid line is a fit to the data using equation (3). (c) fr102cq at $V_L = 0.1$, 0.32, 0.01 and 0.032 µm/s. The solid line is a fit to the data using equation (3).

reference line with zero intercept and a slope of 1, corresponding to $t_r = \Delta\tau/kV_L$. All of the events in these catalogs undergo measureable interseismic slip. Normalizing the data also removes the stressing rate trend kV_L (β_2 from *Karner and Marone* [2000]) and emphasizes the covariances that are observed at constant loading rate (Figures 3 and 4). That is, for example, in the variable loading rate catalog of fr97sq at 10 µm/s and 1 µm/s, there are enough measurements ($N = 30$ and 20, respectively) to resolve the effect at constant loading rate, resulting in low slope trends in the normalized data (Figure 8b).

4. Friction-Based Models of Recurrence

In laboratory friction experiments, two particular fault properties lead to periodic failure at constant loading rate: (1) the steady state fault strength decreases with slip rate [*Dieterich*, 1979]; this allows for the onset of unstable slip and a stress drop and (2) fault strength increases rapidly with time if the sliding velocity is near zero [*Dieterich*, 1972]; this allows the fault to restrengthen immediately following a slip event and for recurrence if the loading rate is lower than the rate of restrengthening. In friction models of these behaviors (rate- and state-dependent friction), both effects are relatable to the steady state rate dependence of the fault strength [*Dieterich*, 1979; *Ruina*, 1983]; that is, the failure strength preceding a stress drop and the sliding strength during the stress drop depend on $(b - a)$ [*Rice and Tse*, 1986; *Scholz et al.*, 1986; *Kanamori and Allen*, 1986; *Cao and Aki*, 1986]. In the following discussion we consider the laboratory stick-slip data sets and how they can be interpreted using the existing rate- and state-dependent constitutive equations. In the immediately following section, we discuss recurrence at variable loading rate, and in the subsequent section, recurrence at constant loading rate.

4.1. Variable Loading Rate

Equation (3) is the relationship governing repeated laboratory failure for rate and state friction [*Gu and Wong*, 1991; *Beeler et al.*, 1998, 2001; *Karner and Marone*, 2000] that has also been used to describe small earthquake recurrence [*Vidale et al.*, 1994; *Marone et al.*, 1995] and, in few instances, large event recurrence [*Cao and Aki*, 1986;

Table 4. Experiments at Different Loading Rates (Brown University)

t_i (s)	τ_i (MPa)	τ_f (MPa)	t_r (s)	$\Delta\tau$ (MPa)	V_L (μm/s)
		Silica Glass fr97sg			
613,805.50	20.064	17.896		2.167	0.100
614,384.06	20.134	17.917	578.56	2.217	0.100
614,931.75	20.125	17.925	547.69	2.200	0.100
615,452.56	19.924	17.992		1.932	0.316
615,608.31	19.939	18.004	155.75	1.935	0.316
615,762.12	19.952	18.007	153.81	1.944	0.316
615,907.44	19.715	18.024		1.691	1.000
615,950.62	19.746	18.023	43.18	1.723	1.000
615,993.69	19.741	18.045	43.07	1.695	1.000
616,037.56	19.759	18.066	43.87	1.693	1.000
616,076.56	19.739	18.062	39.00	1.677	1.000
616,119.56	19.763	18.069	43.00	1.694	1.000
616,162.56	19.767	18.059	43.00	1.708	1.000
616,206.62	19.763	18.062	44.06	1.701	1.000
616,248.62	19.761	18.068	42.00	1.692	1.000
616,290.62	19.743	18.041	42.00	1.702	1.000
616,333.00	19.755	18.053	42.38	1.702	1.000
616,353.38	19.216	18.098		1.118	10.000
616,356.44	19.218	18.099	3.06	1.119	10.000
616,359.62	19.238	18.107	3.18	1.132	10.000
616,362.81	19.245	18.11	3.19	1.135	10.000
616,366.00	19.233	18.121	3.19	1.112	10.000
616,368.88	19.235	18.127	2.88	1.107	10.000
616,371.94	19.257	18.122	3.06	1.135	10.000
616,375.06	19.258	18.117	3.12	1.141	10.000
616,378.38	19.246	18.106	3.32	1.140	10.000
616,381.50	19.243	18.116	3.12	1.127	10.000
616,384.62	19.232	18.116	3.12	1.115	10.000
616,387.81	19.23	18.091	3.19	1.139	10.000
616,390.75	19.214	18.091	2.94	1.123	10.000
616,393.75	19.21	18.093	3.00	1.117	10.000
616,396.81	19.211	18.085	3.06	1.126	10.000
616,399.88	19.217	18.078	3.07	1.139	10.000
616,402.94	19.212	18.088	3.06	1.124	10.000
616,405.88	19.202	18.066	2.94	1.136	10.000
616,409.12	19.208	18.07	3.24	1.138	10.000
616,412.31	19.22	18.074	3.19	1.147	10.000
616,415.25	19.188	18.076	2.94	1.112	10.000
616,418.06	19.181	18.072	2.81	1.108	10.000
616,421.12	19.201	18.073	3.06	1.128	10.000
616,424.31	19.213	18.058	3.19	1.155	10.000
616,427.50	19.206	18.062	3.19	1.143	10.000
616,430.62	19.183	18.059	3.12	1.123	10.000
616,433.75	19.192	18.049	3.13	1.143	10.000
616,436.81	19.178	18.037	3.06	1.141	10.000
616,439.81	19.169	18.042	3.00	1.127	10.000
616,442.75	19.164	18.043	2.94	1.121	10.000
616,445.75	19.176	18.03	3.00	1.146	10.000
616,511.25	19.684	17.98		1.704	1.000
616,555.38	19.696	17.969	44.13	1.727	1.000
616,597.31	19.679	17.999	41.93	1.680	1.000
616,638.31	19.669	17.988	41.00	1.681	1.000
616,682.31	19.687	17.99	44.00	1.698	1.000
616,727.38	19.687	17.971	45.07	1.716	1.000
616,771.31	19.687	17.99	43.93	1.697	1.000
616,814.38	19.692	17.993	43.07	1.700	1.000
408,727.72	19.419	18.241		1.178	10.000
408,730.97	19.39	18.256	3.25	1.134	10.000
408,734.16	19.408	18.272	3.19	1.136	10.000
408,737.22	19.418	18.281	3.06	1.137	10.000

Table 4. (continued)

t_i (s)	τ_i (MPa)	τ_f (MPa)	t_r (s)	$\Delta\tau$ (MPa)	V_L (μm/s)
408,740.41	19.419	18.274	3.19	1.145	10.000
408,743.47	19.419	18.274	3.06	1.144	10.000
408,746.56	19.428	18.279	3.09	1.149	10.000
408,749.72	19.434	18.29	3.16	1.144	10.000
408,753.00	19.455	18.293	3.28	1.162	10.000
408,756.19	19.43	18.284	3.19	1.146	10.000
408,759.47	19.443	18.302	3.28	1.142	10.000
408,762.44	19.442	18.303	2.97	1.139	10.000
408,765.50	19.428	18.295	3.06	1.134	10.000
408,768.66	19.445	18.298	3.16	1.147	10.000
408,771.84	19.442	18.286	3.18	1.156	10.000
408,775.12	19.44	18.277	3.28	1.164	10.000
408,778.12	19.411	18.259	3.00	1.152	10.000
408,781.38	19.413	18.263	3.26	1.150	10.000
408,784.56	19.422	18.27	3.18	1.152	10.000
408,787.53	19.416	18.274	2.97	1.143	10.000
408,790.66	19.424	18.277	3.13	1.146	10.000
408,793.75	19.413	18.256	3.09	1.158	10.000
408,796.94	19.432	18.256	3.19	1.177	10.000
408,800.09	19.41	18.254	3.15	1.155	10.000
408,803.41	19.416	18.255	3.32	1.161	10.000
408,806.66	19.419	18.259	3.25	1.160	10.000
408,809.84	19.417	18.261	3.18	1.156	10.000
408,812.84	19.407	18.247	3.00	1.160	10.000
408,816.00	19.404	18.247	3.16	1.157	10.000
408,819.34	19.414	18.242	3.34	1.172	10.000
408,887.56	19.939	18.203		1.736	1.000
408,930.47	19.932	18.217	42.91	1.715	1.000
408,974.50	19.921	18.212	44.03	1.709	1.000
409,016.47	19.921	18.228	41.97	1.693	1.000
409,059.44	19.916	18.207	42.97	1.709	1.000
409,103.44	19.929	18.21	44.00	1.719	1.000
409,147.41	19.926	18.21	43.97	1.716	1.000
409,189.31	19.91	18.198	41.90	1.713	1.000
409,231.31	19.927	18.212	42.00	1.715	1.000
409,276.28	19.947	18.222	44.97	1.725	1.000
409,321.31	19.929	18.19	45.03	1.738	1.000
409,633.53	20.187	18.214		1.973	0.316
409,788.09	20.181	18.21	154.56	1.971	0.316
409,945.62	20.177	18.212	157.53	1.965	0.316
411,108.88	20.413	18.207		2.206	0.100
411,635.06	20.379	18.184	526.18	2.195	0.100
412,223.25	20.381	18.182	588.19	2.199	0.100
			Quartzite fr102cq		
830,854.10	18.160	16.594			0.010
834,497.82	18.114	16.615	3,643.72	1.499	0.010
838,204.35	18.140	16.611	3,706.53	1.529	0.010
841,837.54	18.155	16.641	3,633.19	1.514	0.010
845,512.60	18.186	16.662	3,675.06	1.524	0.010
848,304.18	18.253	16.680			0.032
849,433.29	18.086	16.671	1,129.11	1.415	0.032
850,541.97	18.119	16.689	1,108.68	1.43	0.032
851,640.32	18.130	16.672	1,098.35	1.458	0.032
852,697.91	18.129	16.682	1,057.59	1.447	0.032
853,757.93	18.135	16.679	1,060.02	1.456	0.032
854,333.00	18.103	16.717			0.100
854,651.48	18.021	16.702	318.48	1.319	0.100
854,974.76	18.034	16.711	323.28	1.323	0.100
855,303.09	18.055	16.691	328.33	1.364	0.100
855,626.61	18.038	16.689	323.52	1.349	0.100
855,944.82	18.050	16.714	318.21	1.336	0.100

10.1002/2014JB011184

Table 4. (continued)

t_i (s)	τ_i (MPa)	τ_f (MPa)	t_r (s)	$\Delta\tau$ (MPa)	V_L (μm/s)
856,160.68	18.054	16.756			0.316
856,242.64	17.872	16.729	81.96	1.143	0.316
856,335.03	17.914	16.729	92.39	1.185	0.316
856,427.50	17.909	16.709	92.47	1.2	0.316
856,520.06	17.883	16.686	92.56	1.197	0.316
856,612.56	17.882	16.687	92.5	1.195	0.316
856,704.98	17.882	16.678	92.42	1.204	0.316

Scholz et al., 1986; *Kanamori and Allen*, 1986; *Scholz*, 1990]. The appropriate constant of proportionality implied by rate and state equations follows from the work of Wong and collaborators [*Gu and Wong*, 1991; *Beeler et al.*, 2001; *He et al.*, 2003], who found that the initial stress increases with recurrence interval (decreasing loading velocity) and that dynamic sliding friction is nearly independent of the recurrence interval. If these properties are applied in a spring slider or a dynamically propagating expanding crack model, slip exceeds that necessary to drop stress to the dynamic strength. Thus, the final arresting stress is lower than the dynamic strength by a fixed amount, a phenomenon that is referred to as "overshoot" [*McGarr*, 1994]. This final stress decreases with recurrence. The net effect is that while neither initial stress nor final stress are independent of recurrence [cf. *Bufe et al.*, 1977; *Shimazaki and Nakata*, 1980], they both vary systematically and the static stress drop follows the logarithmic dependence on recurrence:

$$\Delta\tau(i) = \sigma_n(b-a)(1+\xi)\ln\frac{t_r(i)}{t_0}. \qquad (4)$$

$(b-a)$ is positive [*Ruina*, 1983]. ξ is the fractional overshoot, which for slider block models can be between 0 (final stress is equal to the sliding strength) and 1 (complete overshoot) [*Beeler et al.*, 2001]. Because stress drop is proportional to slip, equation (4) is a nonlinear slip-predictable model of the form shown in Figures 7a, 7b, and 8a.

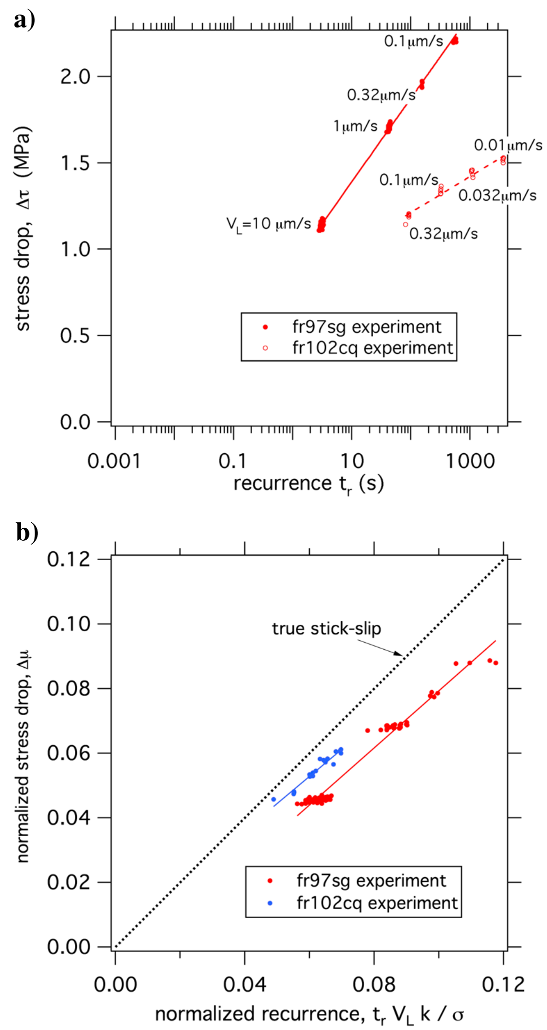

Figure 8. Stress drops over a range of loading rates. (a) Data from silica glass (solid symbols) and quartzite (open symbols) shown in Figures 7a and 7b plotted on semilog axes. The lines are fits to the data with the logarithmic form equation (3). (b) The same data as in Figure 8a plotted as normalized stress drop $\Delta\tau/\sigma_n = \Delta\mu$ and normalized recurrence $t_r V_L k/\sigma_n$ using k/σ_n = 0.002/μm. A reference line with intercept of zero and slope of 1 defines true stick-slip, where there is no slip during the interevent period.

Figure 9a shows the expectations for stress drop and recurrence from rate and state friction using a single degree of freedom slider block. Figure 9b is the normalized version of the same calculations; these are detailed in the Appendix A. To show the relation among friction constitutive parameters, stress drop, and recurrence directly, the acceleration term in the slider block equations [*Johnson and Scholz*, 1976; *Rice and Tse*, 1986] is ignored and motion is damped by radiation losses [*Rice*, 1993]. This leads to no overshoot ($\xi = 0$) and the slope of the plot of stress drop versus $\log_{10}$ recurrence time at large recurrence times is simply related to the steady state rate dependence as $\sigma_n(b-a)$ ln (10) [*Beeler et al.*, 2001]. At short recurrence times the stress drop decreases with decreasing recurrence

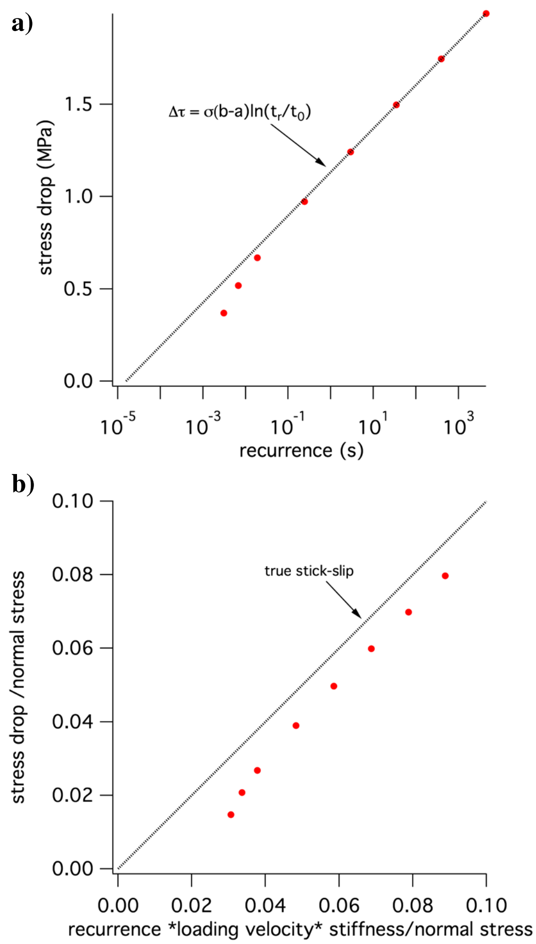

Figure 9. Stress drops over a range of loading rates. (a) Simulations with rate and state friction with $(b-a)=0.004$, $\sigma_n=25$ MPa, $d_c=1$ μm, $k=0.05$ MPa/μm and loading rates of 0.01, 0.1, 1, 10, 100, 1000, 2500, and 5000 μm/s (see Appendix A). The line is a fit to the four lowest loading rates with the logarithmic form equation (4). For these simulations the overshoot is zero, $\xi=0$ in equation (4). (b) The same data as in Figure 9a plotted as normalized stress drop $\Delta\tau/\sigma_n$ and normalized recurrence $t_r V_L k/\sigma_n$. A reference line with intercept of zero and slope of 1 defines true stick-slip, where there is no slip during the interevent period.

more rapidly than predicted by log linear relations. This deviation from the log linear trend results from increased percentages of precursory and afterslip relative to seismic slip. Very low recurrence intervals correspond to high rates of loading and as the duration of loading approaches the duration of the stress drop, the motion becomes oscillatory rather than stick-slip. The values of the constitutive parameters used in simulations are consistent with the experimentally observed values at these loading rates and confirm the validity of equation (4) as an appropriate physical model for laboratory recurrence (Figures 7 and 8) that is empirically well described by equation (3).

4.2. Constant Loading Rate

We also use a slider block model to simulate the covariation of recurrence and stress drop seen in the constant loading rate data (Figures 4–6). The details of the calculations are described in the Appendix A. Because the fault's rate dependence is observed to be the controlling variable in the recurrence model (4), we explore the possibility that slight variations in the rate dependence underlie the covariance of stress drop and recurrence at a single loading rate. Our approach builds on an idea of *Karner and Marone* [2000], namely, that including a stochastic component in a model of periodic slip might account for some of the variability seen in experimental recurrence data. Their approach was to randomly change the value of the state variable during the stress drop. Our calculations are similar to *Karner and Marone* [2000] in using rate and state friction; however, the rate dependence rather than state is changed during the stress drop. The change is made when the slip speed is highest; the rationale also follows *Karner and Marone* [2000], that changes in fault properties would coincide with the most extreme rates of stress and slip change. The values of both a and b are randomly selected from normal distributions. This approach produces a systematic variation of stress drop with recurrence (Figure 10). The covariance is apparent whether the previous or the subsequent stress drop is used, as in the experiments (Figures 4 and 5).

Systematic variations of the failure and final stress with recurrence interval (Figure 6) are also captured in the simulations. Prior and subsequent failure stresses increase with recurrence in the simulations (Figures 11a and 11b, top traces), and prior and subsequent final stresses decrease with recurrence interval (Figures 11a and 11b, lower traces), consistent with the observations. These simulations provide a possible explanation for the observations; however, this may not be a unique explanation and it is possible that unexplored variations in other frictional properties such as state [*Karner and Marone*, 2000] and slip weakening distance may also lead to behavior consistent with the laboratory data.

5. Discussion

Some aspects of why constant rate-loading simulations produce systematic covariation of the failure stress, final stress, and the stress drop with recurrence when the rate dependence, $(b-a)$, is varied are qualitatively

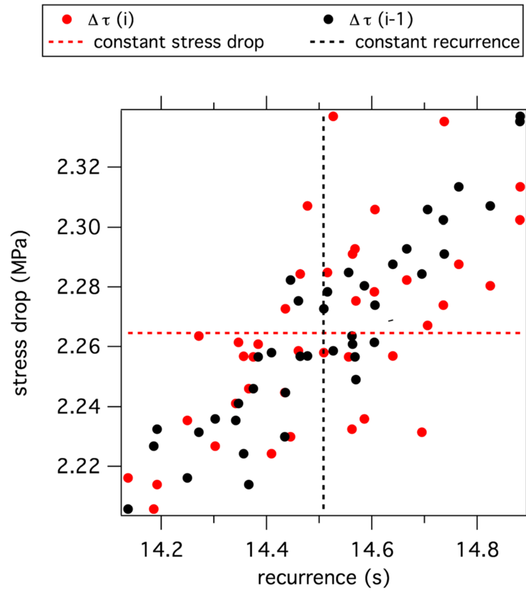

Figure 10. Simulations of stress drop and recurrence at constant loading rate with variable fault rate dependence. Forty-one recurrences from a slider block model with rate and state friction using parameters appropriate for quartzite at 25 MPa normal stress and a loading velocity of 0.3162 μm/s (see Appendix A). The rate and state constitutive parameters, *a* and *b*, used are chosen randomly from normal distributions at the peak velocity during each stress drop. The mean values are $a = 0.008$ and $b = 0.012$ each with standard deviation of 0.7%. Here the simulations are plotted as stress drop versus recurrence (red) and as recurrence versus previous stress drop (black). The data show covariance of stress drop with recurrence regardless of whether the stress drop or previous stress drop are considered, as seen in the experiments (compare with Figures 4 and 5).

explained by analogy to the numerical studies of periodic slip with rate and state friction by *He et al.* [2003] and *Beeler et al.* [2001]. In summary, these studies show that stress drop decreases with loading rate, equivalently increases with recurrence interval, as in equation (3), by an amount controlled by $(b - a)$. In detail, the change in stress drop corresponds to changes in both the failure and final stresses, increases, and decreases, respectively, when the recurrence interval is increased. Keeping these systematics in mind, we can apply these results to the case of a change in $(b - a)$ at constant loading rate. Say, for example, that during a stress drop the rate dependence $b - a$ increases. If fault slip overshoots as it does in the simulations, this corresponds to a lower value of the final stress because the final stress depends on recurrence as $\sigma_n (a - b) (\xi) \ln t_r$ [*He et al.*, 2003; *Beeler et al.*, 2001]. This lower value of the final stress, the starting stress for the subsequent reload, increases the subsequent recurrence interval because it takes longer to reload to the next peak stress. This explains the interdependence between recurrence and the prior value of the final stress (Figure 11b, lower trace). The increase in the subsequent recurrence time corresponds to a slight increase in the failure stress as the failure stress also depends on the logarithm of the loading time as on $\sigma_n (b - a)$, explaining the relation between the peak stress and the recurrence interval (Figure 11a, upper trace).

The other aspects of the simulations, the relation between final stress and the prior recurrence interval (Figure 11a, lower trace), and failure stress on the subsequent recurrence interval (Figure 11b, upper trace) seem to result from more extended memory effects. For example, continuing to consider the example discussed in the previous paragraph, where $(b - a)$ is increased during a stress drop, if $(b - a)$ then remained constant through the next stress drop, there would be a similar relationship between the final stress and the prior recurrence interval as between the failure stress and the prior recurrence. That is, the failure stress scales as $\sigma_n (b - a) \ln t_r$ and the final stress as $\sigma_n (a - b) (\xi) \ln t_r$ [*He et al.*, 2003; *Beeler et al.*, 2001]. In the actual simulations, the rate dependence is changed during this stress drop, and yet there is a muted relationship (Figure 11a, lower trace) between the resulting final stress and the prior recurrence interval that is consistent with the expected result had the rate dependence not changed, indicating some memory of the prior value of $(b - a)$, or equivalently reflecting that the peak stress was high prior to the change in $(b - a)$. This kind of longer-term memory also qualitatively explains the relation between the prior failure stress and the subsequent recurrence interval (Figure 11b, upper trace).

That said, in some cases the details of the simulations are different from the observations, for example, in the experiments the slope of stress drop versus recurrence is lower than the stressing rate line (grey dashed lines in Figures 4, 5b, and 5c), whereas the slope in the simulations is indistinguishable from the stressing rate. Apparently, there is a weaker relationship between these two quantities in the experiments, there is an additional systematic source of uncertainty not accounted for in the simulations, or the particular constitutive relationships used are not entirely appropriate. Understanding the origin of this difference is particularly important because any relation between prior stress drop and subsequent recurrence interval, a general time predictability, is potentially useful in prospective forecasting of earthquake recurrence and failure time. Empirical relationships might be established in more extensive continuous experimental catalogs.

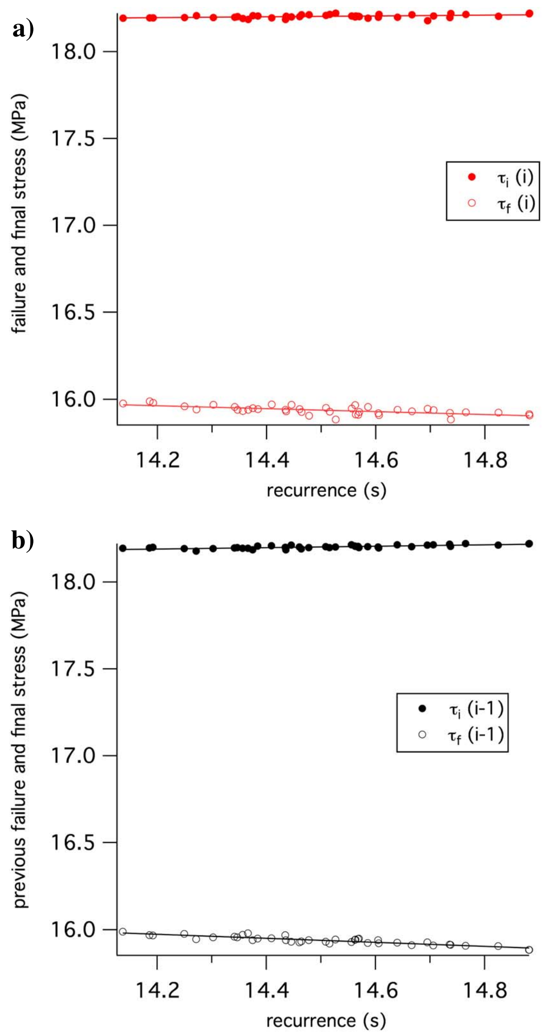

Figure 11. Variation of initial and final stresses with recurrence at constant loading rate with variable fault rate dependence. These are the same simulations as in Figure 10. (a) The initial and final stresses defining the stress drop $\Delta\tau(i)$ following recurrence interval $t_r(i)$. The lines are fits to the simulations. Both show weak dependence: an increase in the initial strength with recurrence and a decrease in final stress with recurrence, qualitatively similar to the experimental observations (Figure 6a). (b) The initial and final stresses defining the stress drop $\Delta\tau(i-1)$ preceding the recurrence interval $t_r(i)$. The lines are fits to the data. As in Figure 11a, both stresses show correlation with recurrence interval: an increase in the initial strength with recurrence and a decrease in final stress with recurrence, qualitatively similar to the observations (Figure 6b).

While the existing strict time predictable, slip predictable, and constant stress drop/constant recurrence characteristic models are all ruled out by the experiments presented in this study, the catalogs are at least to second-order characteristic, with low order, more general time, and slip-predictable properties. According to our arguments all of these tendencies result from the rate dependence of fault strength. For consideration of different loading rates, the relationship (4) or (3) fits the experimental observations and cases of natural earthquake recurrence [*Cao and Aki*, 1986; *Scholz et al.,* 1986; *Kanamori and Allen*, 1986], in particular, where the loading rate is varied, presumably by afterslip: *Schaff et al.* [1999], *Vidale et al.* [1994], *Marone et al.* [1995], and *Beeler et al.* [2001]. This relationship should also apply during natural constant rate loading under certain circumstances; for example, equation (4) could be combined with a stochastic component based on laboratory variance from constant loading rate experiments (Figures 4 and 5) to estimate recurrence probability following a main shock. Using such a model will produce immediately post-main-shock recurrence probabilities that are effectively zero, due to the rapid restrengthening observed in laboratory studies [*Dieterich*, 1972]. More generally, including uncertainties of the constitutive properties in deterministic models should allow more direct application to natural occurrence than perfectly periodic rate- and state-dependent friction models.

5.1. Future Laboratory Work and Application to Natural Faulting

If prior stress drop influences the recurrence interval and if recurrence interval influences the subsequent stress drop as implied by Figures 4–6, then successive stress drops should covary. Indeed, in the continuous catalog fr116cq ($N = 33$), prior and subsequent stress drops $\tau(i-1)$ and $\tau(i)$ are quite strongly correlated (Figure 12). The linear covariance is $r = 0.62$; there is only a 0.014% chance that uncorrelated data would result in a covariance this large or larger. This implies that during recurrence cycles, fault strength has an extended memory of prior slip history that may be expected from rate- and state-dependent friction [*Ruina*, 1983]; this behavior is also captured in the same simulation shown in Figures 10 and 11 (Figure A1). Possibly related effects arise in some multicycle dynamic rupture simulations [*Radiguet et al.,* 2013]. While it may be that these longer-term correlations extend even further in time than a single cycle in the experiments, those details are beyond the scope of the present study. A larger concern is whether such memory effects could occur at natural loading rates and recurrence intervals. The loading rates used to generate the experimental catalogs are between 0.32 and 10 μm/s, roughly 300 to 10,000 times larger than the long-term slip rate of the San Andreas. The recurrence intervals are between a few and about 150 s, so “memory” is not an appreciable amount of time relative to the cycle of even the smallest

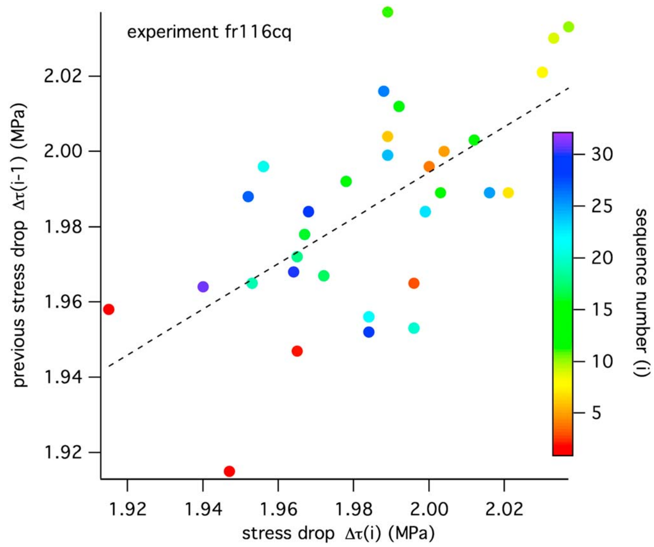

Figure 12. Covariance of prior stress drop $\tau(i-1)$ with stress drop $\tau(i)$ from the experiment fr116cq. Dashed line is a fit to the data. Data are color coded by sequence number (i) to indicate order within the catalog.

repeating earthquakes. Short recurrence times of repeating earthquakes on the San Andreas are around 1 year [e.g., *Nadeau and Johnson*, 1998], more than 5 orders of magnitude longer than the longest recurrences in the experiments. While the equations used in the simulations in this paper could be used to extrapolate the effects, it would be more convincing and more appropriate to conduct experiments that determine whether these effects arise at recurrence times that are orders of magnitude longer than in the present study. So some careful experiments are needed to ensure that the memory effects seen in experiments extrapolate in both loading rate and stiffness, i.e., in stressing rate $\dot{\tau} = kV_L$.

Related to issues of extrapolation is the size of the covariances seen in the constant loading rate experiments, relative to the documented variability seen in natural settings. In these experiments, covariance of stress drop with recurrence and cycle duration memory effects are only established in highly periodic, very low variance catalogs with large numbers of recurrences. Because of the large numbers and small uncertainties, it may be that whether such effects occur in natural catalogs cannot be resolved due to other much larger natural sources of variability. Comprehensive analysis of natural sequences is needed. On the other hand, if the covariance arises from uncertainty in the steady state rate dependence, as in our simulations, it is possible and perhaps more likely that such variations are larger in natural settings due to material heterogeneity, variable influences of chemical environment, etc. and that covariance and memory effects are more robust in natural sequences. More extensive numerical calculations could be used to better understand issues associated with extrapolation.

A final concern about the applicability of these laboratory results involves the physical mechanism. The underlying rate-dependent effects that lead to the stress drop in the experiments also control the size of the eventual stress drop and therefore how that stress drop changes with loading rate as well as all of the other details that manifest as covariance between stress drop and recurrence, and as memory effects. In natural settings, even for very small repeating earthquakes, the slip and slip rates during stress drop are much higher than in the lab. The higher slips and slip rates may cause shear heating sufficient to change the mechanism that controls dynamic strength. Under those circumstances, the relationships between stress drop and recurrence are expected to be very different than in the present experiments. For the simple recurrence model (4), initial stress is related to the steady state rate dependence and the final strength to the rate dependence via an overshoot parameter. For shear-heating-induced dynamic weakening the initial stress will follow scaling consistent with (4), but the dynamic sliding strength is much lower and the degree of overshoot may in some cases be determined by the fault strength itself rather than by inertial effects [e.g., *Beeler*, 2006]. At present, verified constitutive relationships for dynamic weakening are only available for shear melting and flash weakening [*Nielsen et al.*, 2008, 2010; *Rice,* 2006]. Some implications of these for recurrence might be explored in numerical and theoretical studies.

6. Conclusions

In earthquake recurrence experiments, constant rate loading of bare rock surfaces produces deviations from a perfectly periodic model that are second order or smaller. When loading rate is varied, recurrence is approximately inversely proportional to loading rate. Laboratory events initiate due to slip-rate-dependent processes that also determine the size of the stress drop and, as a consequence, laboratory data sets show

10.1002/2014JB011184

that stress drop varies weakly but systematically with loading rate. Experimentally observed stress drops are well described by a recurrence model containing a logarithmic dependence on recurrence interval, where the fault's rate dependence of strength is the key controlling physical parameter. Laboratory recurrence is not exactly periodic; even at constant loading rate, stress drop and recurrence interval covary systematically. The covariance is consistent with variations of the fault's rate dependence of strength. Recurrence shows aspects of both time and slip predictability, and stress drop correlates strongly with the previous stress drop, indicating an earthquake-cycle-long memory of prior slip history.

Appendix A: Simulations of the Experiments

For simulation of periodic slip with rate and state friction we use a single degree of freedom spring slider block [*Johnson and Scholz*, 1976; *Rice and Tse*, 1986]. The equation of motion can be expressed as the balance of the mass times acceleration against the difference between the spring force (here expressed as having units of stress) and the frictional resisting stress, less the radiated energy,

$$\left(\frac{T}{2\pi}\right)^2 \frac{\mathrm{d}V}{\mathrm{d}t} = (\delta_L - \delta) - \frac{\tau}{k} - \frac{\chi}{k}\frac{\partial\delta}{\partial t}. \tag{A1}$$

T is the characteristic period of oscillation, $T = \sqrt{m/Ak}$ where m is mass, A is fault area, and k is the elastic shear stiffness of the fault (in units stress/displacement); δ is slip on the fault, δ_L is load point displacement, the shear resistance or fault strength is τ, $\chi = \mu/2\beta$, where β is the wave speed and μ is the shear modulus. The spring force, equivalent to the fault shear stress, is $k(\delta_L - \delta)$. The radiation damping term $\chi \mathrm{d}\delta/\mathrm{d}t$ is used to approximate energy lost as propagating seismic waves, here assumed to be planar waves [*Rice*, 1993]. The particular choice χ is appropriate if β is the shear wave speed and all radiation results from shear waves [*Rice*, 1993].

The fault strength is attributed to rate and state friction using the particular formulation following *Rice and Tse* [1986]:

$$\tau = \sigma_n(f_o + a\ln\,(V/V_0) + \theta) \tag{A2a}$$

$$\frac{\mathrm{d}\theta}{\mathrm{d}t} = -\frac{V}{d_c}\left(\theta + b\ln\frac{V}{V_0}\right), \tag{A2b}$$

$$\frac{\mathrm{d}\theta}{\mathrm{d}t} = \frac{b}{d_c}\left(V_0 \exp\;\frac{-\theta}{b} - V\right) \tag{A2c}$$

where f_0 is a constant, a and b are second-order constants relative to f_0, V is slip speed, V_0 is a reference slip speed, d_c is a characteristic length scale, and σ_n is normal stress; θ is a state variable with the possible physical interpretation of fractional contact area on the sliding surface [*Dieterich*, 1979]. Equations (A2b) and (A2c) are two proposed representations of the state variable [*Ruina*, 1983].

Two different types of simulations are done in this study: (1) constant loading rate with varying fault properties and (2) constant fault properties over a range of loading rates. To simulate recurrence at constant loading rate, equation (A1) was used. To illustrate the relationship between stress drop and recurrence for rate and state friction at simulations over a wide range of loading velocities, for simplicity, the inertial term is ignored and radiation losses limit the motion.

A1. Variable Loading Rate and Constant Fault Properties

The equation of motion used is (A1) with no acceleration:

$$(\delta_L - \delta) = \frac{\tau}{k} + \frac{\chi}{k}\frac{\partial\delta}{\partial t}. \tag{A3}$$

This approach produces no dynamic overshoot; that is, slip arrests when the spring force drops to the level of the sliding resistance. Simulations were conducted at a range of loading rates. At each rate, the spring load point is displaced at V_L, resulting in a sequence of periodic slip events. The recurrence time is measured from successive values of the peak strength, and the stress drop is the difference between the peak and final stresses, as in the experimental measurements (Figure 1). Simulations were conducted at 0.1, 1, 10, 100, 1000, 2500, and 5000 μm/s. The results of these calculations are shown in Figure 9.

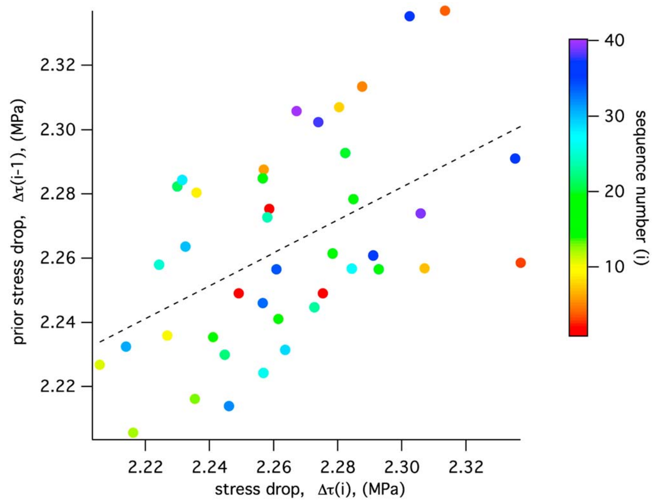

Figure A1. Simulated covariance of prior stress drop $\tau(i-1)$ with stress drop $\tau(i)$ from the same calculation shown in Figures 10 and 11. Dashed line is a fit to the simulations. Each event in the sequence is color coded by sequence number (i) to indicate order within the catalog.

A2. Constant Loading Rate and Variable Fault Properties

The equation of motion used is (A1). Simulations were conducted at a single loading velocity $V_L = 0.3162$ μm/s, $V_0 = 3.162$ μm/s, $d_c = 1$ μm, $f_0 = 0.7$, $k = 0.0525$ MPa/μm, and $\sigma_n = 25$ MPa. Because equations (A1) and (A2a), (A2b), (A2c) have intrinsic time constants that are different by many orders of magnitude, these must be solved using time steps appropriate for the smallest time constant [*Rice and Tse*, 1986]. The calculations use the state variable equation (A2c). To make the numerical calculations faster we have used a value of $T = 0.1$ s, which is likely to be orders of magnitude higher than the characteristic period of the testing machine. This causes the motion to be inertia limited and produce complete overshoot, whereas the overshoot in the experiments is not known. To simulate the effect of variability in the rate dependence on stress drop and recurrence at a constant loading rate, the parameters defining the rate dependence, a and b, were each changed a small amount once per cycle to values selected randomly from a normal distribution. For a the mean of the distribution is 0.008, and the standard deviation is 0.7% of the mean. For b the mean of the distribution is 0.012, and the standard deviation is 0.7% of the mean. The parameters a and b were changed during each stress drop at the time when $dV/dt = 0$, the slip rate is at its maximum and approximately one half of the slip during the stress drop has already occurred. The motivation for choosing this particular time to change the rate dependence follows *Karner and Marone* [2000]; this is the time when rates of slip and stress change are at their maximums and thus the most likely time for the fault to change its properties; it is otherwise an ad hoc choice. The other parameters used in the simulations are consistent with the apparatus elastic properties, normal stress, and the frictional properties of quartzite. The results of the simulations shown in Figures 10, 11 and A1 indicate that small changes in these constitutive parameters lead to systematic changes in the failure stress, final stress, stress drop, and recurrence interval during constant rate loading that are of the same sense and qualitatively similar to those seen in the experiments. In particular, the previous stress drop correlates with stress drop (Figure A1) capturing the cycle-long memory observed in the experiments (Figure 12).

Acknowledgments

Data used in the figures and analysis are found in the Tables 1–4. The large untabled data set from fr97sg is available from the corresponding author (N.M.B.). The particular experimental procedures used were developed by John D. Weeks. The experiments were conducted by J.D.W. and N.M.B. Telemaco Tesei pointed out the earlier numerical study by Radiquet et al., in which memory effects have been reported. The analysis used here was developed during a project studying stick-slip at high loading rates with Giulio Di Toro under a 2007 European Research Council Starting grant: Uncovering the secrets of an earthquake, and in a Southern California Earthquake Center grant 04097 on dynamic rupture and earthquake recurrence to Brown University. SCEC is presently funded by NSF Cooperative agreement EAR-0529922 and USGS Cooperative agreement 07HQAG0008. The SCEC contribution number for this paper is 1811. David Lockner and Greg McLaskey of the USGS, and Chris Marone and an anonymous JGR referee provided reviews that significantly improved the manuscript.

References

Beeler, N. M. (2006), Inferring earthquake source properties from laboratory observations and the scope of lab contributions to source physics, in *Earthquakes: Radiated Energy and Earthquake Physics*, *Geophys. Monogr. Ser.*, vol. 170, edited by R. Abercrombie et al., pp. 99–119, AGU, Washington, D. C.

Beeler, N. M., T. E. Tullis, M. L. Blanpied, and J. D. Weeks (1996), Frictional behavior of large displacement experimental faults, *J. Geophys. Res.*, *101*, 8697–8715, doi:10.1029/96JB00411.

Beeler, N. M., T.-F. Wong, and S. H. Hickman (1998), Stress drop and interseismic strength recovery, *Eos Trans. AGU*, *79*, 224, doi:10.1029/98EO00372.

Beeler, N. M., T.-F. Wong, and S. H. Hickman (2001), Stress drop and laboratory-inferred interseismic strength recovery, *J. Geophys. Res.*, *106*, 30,701–30,713, doi:10.1029/2000JB900242.

Beeler, N. M., B. Kilgore, A. McGarr, J. Fletcher, J. Evans, and S. R. Baker (2012), Observed source parameters for dynamic rupture with non-uniform initial stress and relatively high fracture energy, *J. Structural Geol.*, *38*, 77–89.

Brace, W. F., and J. D. Byerlee (1966), Stick slip as a mechanism for earthquakes, *Science*, *153*, 990–992.

Bufe, C. G., P. W. Harsh, and R. O. Burford (1977), Steady-state seismic slip—A precise recurrence model, *Geophys. Res. Lett.*, *4*, 91–94, doi:10.1029/GL004i002p00091.

Cao, T., and K. Aki (1986), Effect of slip rate on stress drop, *Pure Appl. Geophys.*, *124*, 515–530.

Dieterich, J. H. (1972), Time-dependent friction in rocks, *J. Geophys. Res.*, *77*, 3690–3697, doi:10.1029/JB077i020p03690.

Dieterich, J. H. (1979), Modeling of rock friction: 1. Experimental results and constitutive equations, *J. Geophys. Res.*, *84*, 2161–2168, doi:10.1029/JB084iB05p02161.

Dieterich, J. H. (1981), Potential for geophysical experiments in large scale tests, *Geophys. Res. Lett.*, *8*, 653–656, doi:10.1029/GL008i007p00653.

Ellsworth, W. L. (1995), Characteristic earthquakes and long-term earthquake forecasts: Implications of central California seismicity, in *Urban Disaster Mitigation: The Role of Science and Technology*, edited by F. Y. Cheng and M. S. Sheu, pp. 1–14, Elsevier, Oxford.

Field, E. H., et al. (2008), The uniform California earthquake rupture forecast, version 2 (UCERF2), *U.S. Geol. Surv. Open File Rep., 2007-1437*.

Gu, Y., and T.-F. Wong (1991), Effects of loading velocity, stiffness and inertia on the dynamics of a single degree of freedom spring-slider system, *J. Geophys. Res.*, *96*, 21,677–21,691, doi:10.1029/91JB02271.

He, C., T.-F. Wong, and N. M. Beeler (2003), Scaling of stress drop with recurrence interval and loading velocity for laboratory-derived fault strength relations, *J. Geophys. Res.*, *108*(B1), 2037, doi:10.1029/2002JB001890.

Hecker, S., N. A. Abrahamson, and K. E. Wooddell (2013), Variability of displacement at a point: Implications for earthquake-size distribution and rupture hazards on faults, *Bull. Seismol. Soc. Am.*, *103*, 651–674.

Johnson, T., and C. Scholz (1976), Dynamic properties of stick-slip friction of rock, *J. Geophys. Res.*, *81*, 881–888, doi:10.1029/JB081i005p00881.

Junger, J., B. Kilgore, N. M. Beeler, and J. Dieterich (2004), Earthquake prediction in large-scale faulting experiments, Abstract NG54A-07 presented at 2004 AGU Fall Meeting.

Kanamori, H., and C. R. Allen (1986), Earthquake repeat time and average stress drop, in *Earthquake Source Mechanics*, *Geophys. Monogr. Ser.*, vol. 37, edited by S. Das et al., pp. 227–236, AGU, Washington, D. C.

Karner, S. L., and C. Marone (2000), Effects of loading rate and normal stress on stress drop and stick-slip recurrence interval, in *Geocomplexity and the Physics of Earthquakes*, *Geophys. Monogr. Ser.*, vol. 120, edited by J. B. Rundle et al., pp. 187–198, AGU, Washington, D. C.

Kilgore, B., and N. M. Beeler (2010), Evaluating earthquake 'predictions' on laboratory experiments and resulting strategies for 'predicting' natural earthquake recurrence, *Seismol. Res. Lett.*, *81*(2), 361.

Marone, C., J. E. Vidale, and W. L. Ellsworth (1995), Fault healing inferred from time dependent variations in source properties, *Geophys. Res. Lett.*, *22*, 3095–3098, doi:10.1029/95GL03076.

McGarr, A. (1994), Some comparisons between mining-induced and laboratory earthquakes, *Pure Appl. Geophys.*, *142*, 467–489.

McLaskey, G. C., A. M. Thomas, S. D. Glazer, and R. M. Nadeau (2012), Fault healing promotes high-frequency earthquakes in laboratory experiments and on natural faults, *Nature*, *491*, 101–105, doi:10.1038/nature11512.

Nadeau, R. M., and L. R. Johnson (1998), Seismological studies at Parkfield VI: Moment release rates and estimates of source parameters for small repeating earthquakes, *Bull. Seismol. Soc. Am.*, *88*, 790–814.

Nielsen, S., G. Di Toro, T. Hirose, and T. Shimamoto (2008), Frictional melt and seismic slip, *J. Geophys. Res.*, *113*, B01308, doi:10.1029/2007JB005122.

Nielsen, S., P. Mosca, G. Giberti, G. Di Toro, T. Hirose, and T. Shimamoto (2010), On the transient behavior of frictional melt during seismic slip, *J. Geophys. Res.*, *115*, B10301, doi:10.1029/2009JB007020.

Okubo, P. G., and J. H. Dieterich (1984), Effects of physical fault properties on frictional instabilities produced on simulated faults, *J. Geophys. Res.*, *88*, 887–890.

Page, M. T., D. Alderson, and J. Doyle (2011), The magnitude distribution near southern California fault, *J. Geophys. Res.*, *116*, B12309, doi:10.1029/2010JB007933.

Petersen, M. D., et al. (2008), Documentation for the 2008 update of the United States national seismic hazard maps, *U.S. Geol. Surv. Open File Rep., 2008-1128*, 60 pp.

Power, W. L., T. E. Tullis, and J. D. Weeks (1988), Roughness and wear during brittle faulting, *J. Geophys. Res.*, *98*, 15,268–15,278, doi:10.1029/JB093iB12p15268.

Radiguet, M., D. S. Kammer, P. Gillet, and J.-F. Molinari (2013), Survival of heterogeneous stress distributions created by precursory slip at frictional interfaces, *Phys. Rev. Lett.*, *111*, doi:10.1103/PhysRevLett.111.164302.

Rice, J. R. (1993), Spatio-temporal complexity of slip on a fault, *J. Geophys. Res.*, *98*, 9885–9907, doi:10.1029/93JB00191.

Rice, J. R. (2006), Heating and weakening of faults during earthquake slip, *J. Geophys. Res.*, *111*, B05311, doi:10.1029/2005JB004006.

Rice, J. R., and S. T. Tse (1986), Dynamic motion of a single degree of freedom system following a rate and state dependent friction law, *J. Geophys. Res.*, *91*, 521–530, doi:10.1029/JB091iB01p00521.

Rubinstein, J. L., W. L. Ellsworth, K. Chen, and N. Uchida (2012a), Fixed recurrence and slip models better predict earthquake behavior than the time- and slip-predictable models: 1. Repeating earthquakes, *J. Geophys. Res.*, *117*, B02306, doi:10.1029/2011JB008724.

Rubinstein, J. L., W. E. Ellsworth, N. M. Beeler, B. D. Kilgore, D. A. Lockner, and H. M. Savage (2012b), Fixed recurrence and slip models better predict earthquake behavior than the time- and slip-predictable models: 2. Laboratory earthquakes, *J. Geophys. Res.*, *117*, B02307, doi:10.1029/2011JB008723.

Ruina, A. L. (1983), Slip instability and state variable friction laws, *J. Geophys. Res.*, *88*, 10,359–10,370, doi:10.1029/JB088iB12p10359.

Schaff, D. P., G. C. Beroza, and B. E. Shaw (1999), Post seismic response of repeating aftershocks, *Geophys. Res. Lett.*, *25*, 4549–4552, doi:10.1029/1998GL900192.

Scholz, C. H. (1990), *The Mechanics of Earthquakes and Faulting,* 439 pp., Cambridge Univ. Press, Cambridge, U. K.

Scholz, C. H., C. A. Aviles, and S. G. Wesnousky (1986), Scaling differences between large interplate and intraplate earthquake, *Bull. Seismol. Soc. Am.*, *76*, 65–70.

Schwartz, D. P., and K. J. Coppersmith (1984), Fault behavior and characteristic earthquakes: Examples from the Wasatch and San Andreas fault zones, *J. Geophys. Res.*, *89*, 5681–5698, doi:10.1029/JB089iB07p05681.

Schwartz, D. P., K. J. Coppersmith, F. K. Swan III, P. Somerville, and W. U. Savage (1981), Characteristic earthquakes on intraplate normal faults, *Earthquake Notes*, *52*, 71.

Shimazaki, K., and T. Nakata (1980), Time-predictable recurrence model for large earthquakes, *Geophys. Res. Lett.*, *7*, 279–282, doi:10.1029/GL007i004p00279.

Taylor, J. R. (1997), *An Introduction to Error Analysis*, 327 pp., Univ. Science, Sausalito, Calif.

Thomas, A. M., R. Burgmann, D. R. Shelly, N. M. Beeler, and M. L. Rudolph (2012), Tidal sensitivity of low frequency earthquakes near Parkfield, CA: Implications for fault mechanics within the brittle-ductile transition, *J. Geophys. Res.*, *117*, B05301, doi:10.1029/2011JB009036.

Tullis, T. E., and J. D. Weeks (1986), Constitutive behavior and stability of frictional sliding of granite, *Pure Appl. Geophys.*, *124*, 384–414.

Uchida, N., A. Hasegawa, T. Matsuzawa, and T. Igarashi (2004), Pre- and post-seismic slow slip on the plate boundary off Sanriku, NE Japan associated with three interplate earthquakes as estimated from small repeating earthquake data, *Tectonophysics*, *385*, 1–15.

Vidale, J. E., W. L. Ellsworth, A. Cole, and C. Marone (1994), Variations in rupture process with recurrence interval in a repeated small earthquake, *Nature*, *368*, 624–626.

Wallace, R. E. (1970), Earthquake recurrence intervals on the San Andreas fault, *Geol. Soc. Am. Bull.*, *81*, 2875–2890.

Weeks, J. D., N. M. Beeler, and T. E. Tullis (1991), Glass is like a rock, *Eos Trans. AGU*, *72*, 457–458.

Wesnousky, S. G. (1994), The Gutenberg-Richter or characteristic distribution, which is it?, *Bull. Seismol. Soc. Am.*, *84*, 1940–1959.

Wesnousky, S. G. (1996), Reply to Yan Kagan's comment on "The Gutenberg-Richter or characteristic distribution, which is it?", *Bull. Seismol. Soc. Am.*, *85*, 286–291.

Wong, T.-F., and Y. Zhao (1990), Effects of load point velocity on frictional instability behavior, *Tectonophysics*, *175*, 177–195.